Quantum dynamics of entanglement and hadronization in jet production in the massive Schwinger model

David Frenklakh

Brookhaven National Laboratory

2301.11991, 2404.00087

[Florio, DF, Ikeda, Kharzeev, Korepin, Shi, Yu]

+ work in progress

with A.Florio, S.Grieninger, D.Kharzeev,

A. Palermo and S. Shi

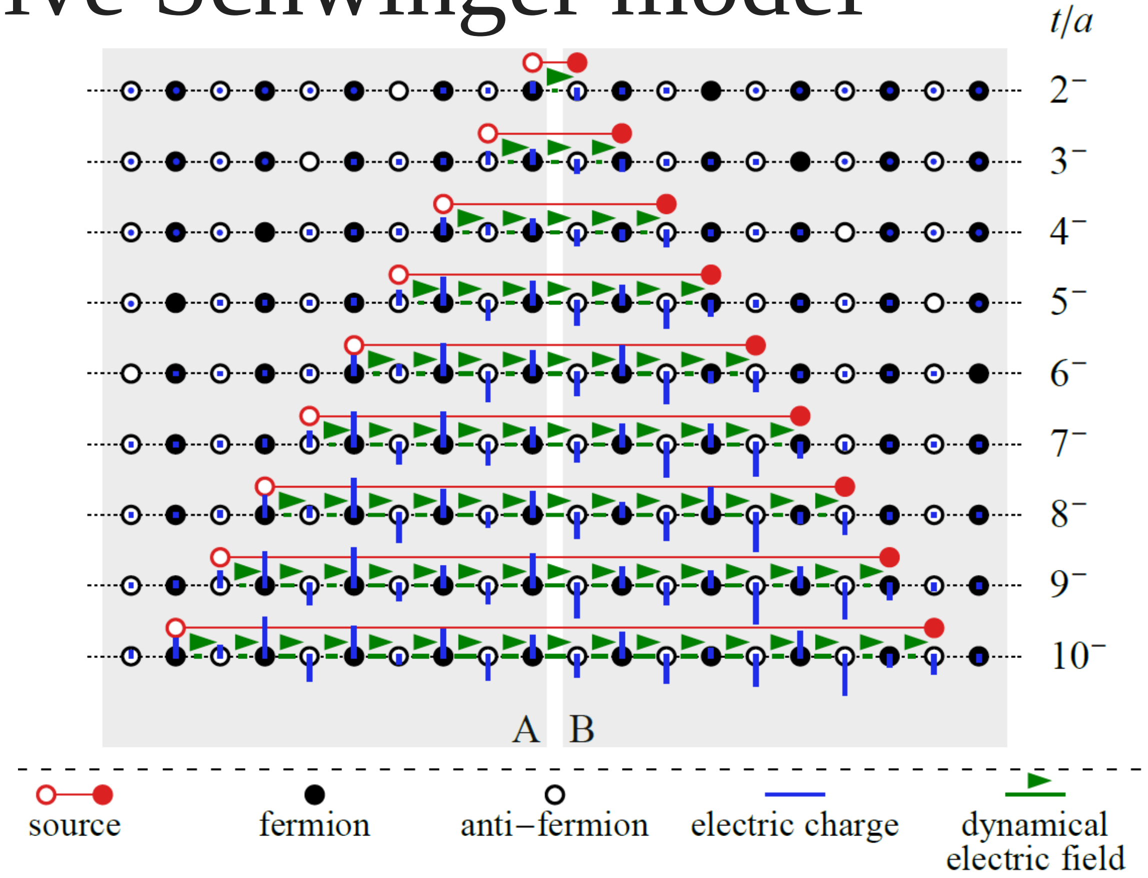

CFNS Workshop *Probing the frontiers of nuclear physics with AI at the EIC (II)*

Stony Brook 3.19.2025

Motivation

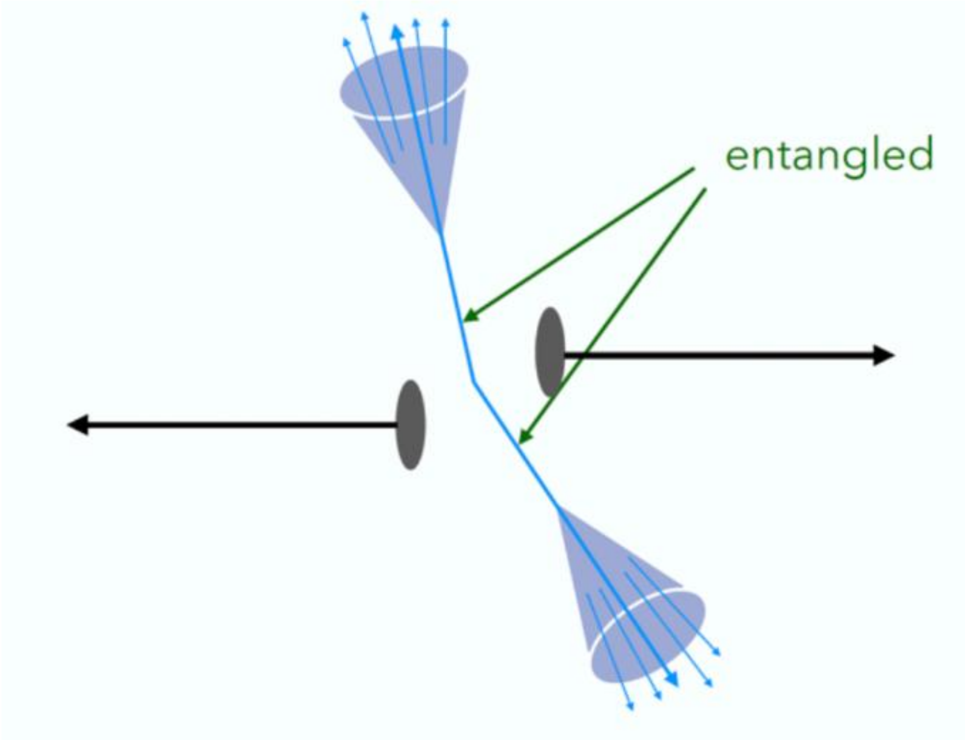

Originating in the same process, the partons possess quantum entanglement.

Motivation

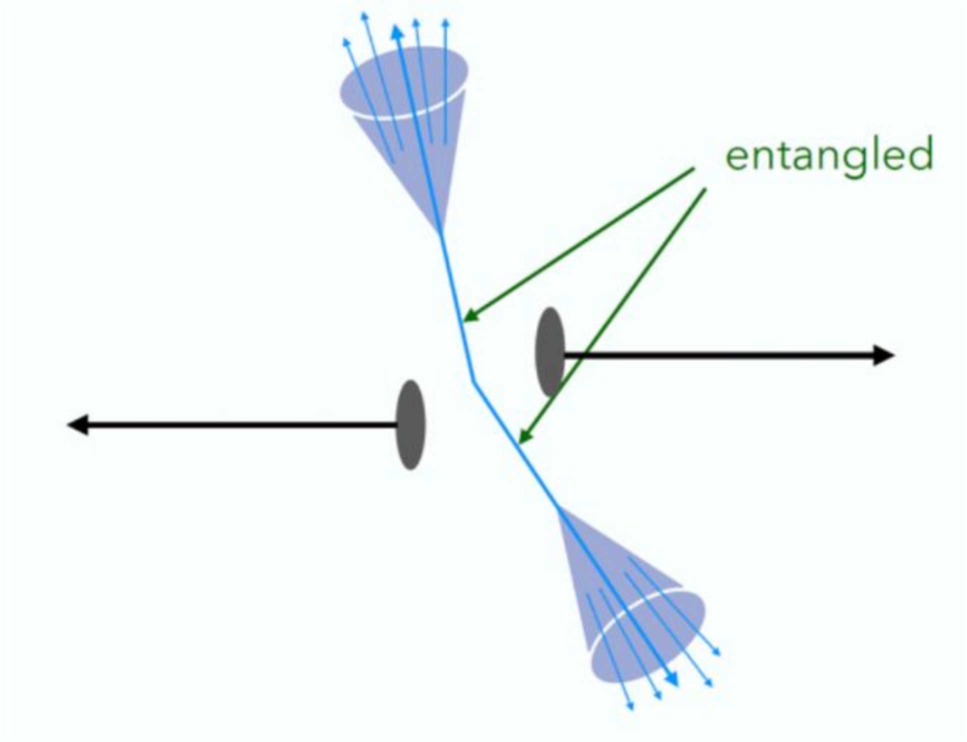

Originating in the same process, the partons possess quantum entanglement.

(Recent explorations of entanglement in DIS [Kharzeev, Levin ’17], [Kharzeev ’21])

Motivation

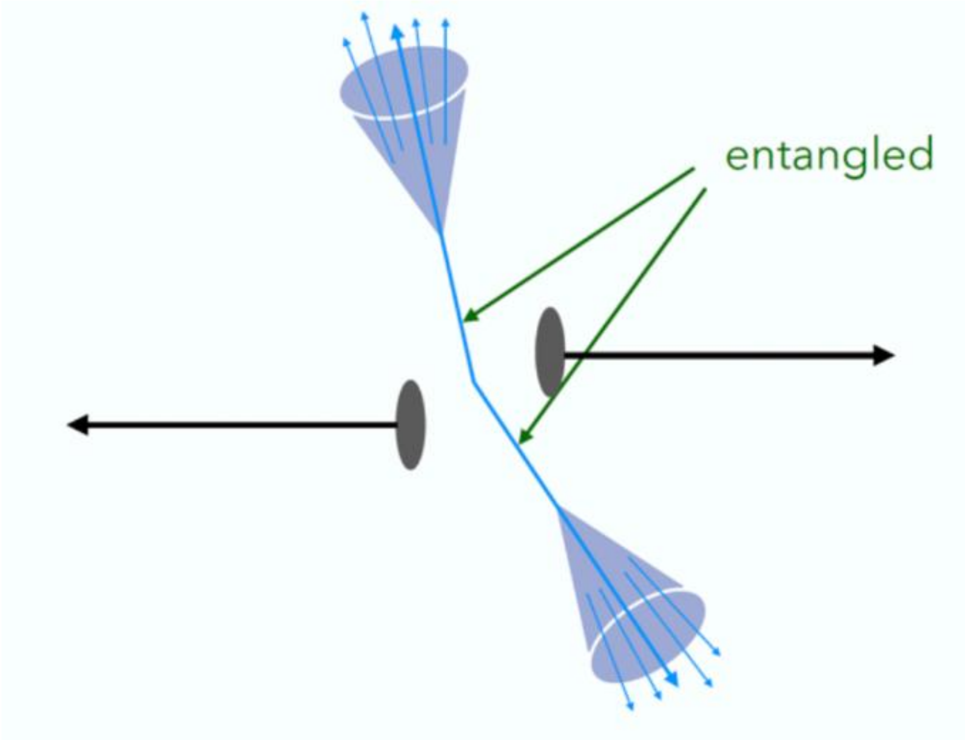

Originating in the same process, the partons possess quantum entanglement.

(Recent explorations of entanglement in DIS [Kharzeev, Levin ’17], [Kharzeev ’21])

Real-time quantum process requires

Real-time quantum simulation

Motivation

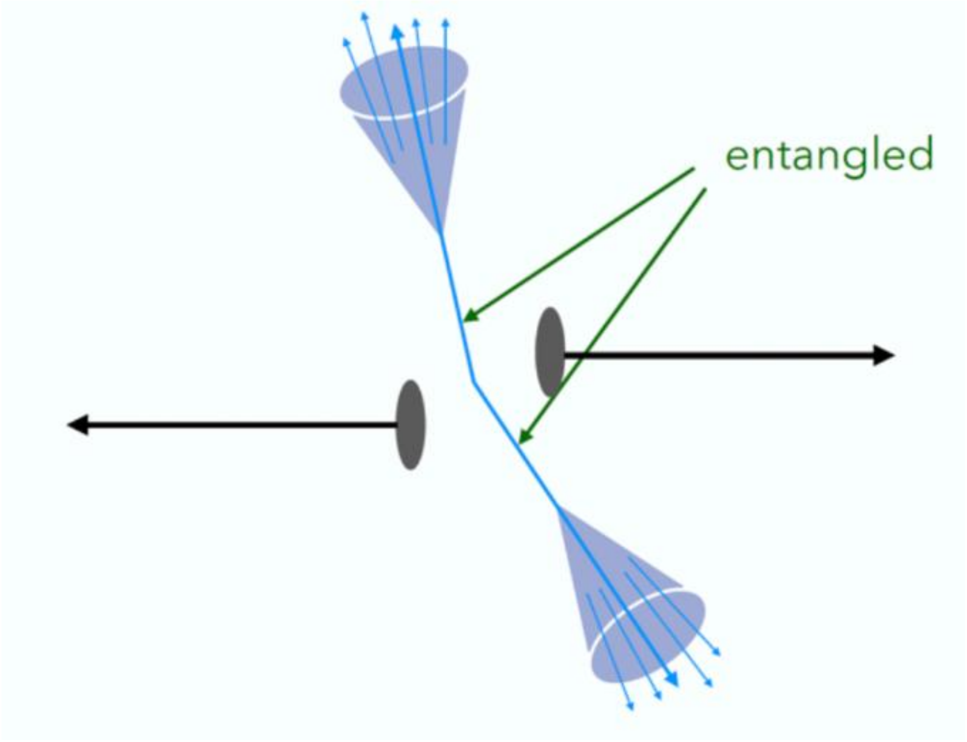

Originating in the same process, the partons possess quantum entanglement.

(Recent explorations of entanglement in DIS [Kharzeev, Levin ’17], [Kharzeev ’21])

Real-time quantum process requires

Real-time quantum simulation

Testbed for learning
interesting physics with methods
suitable for quantum simulation

Motivation

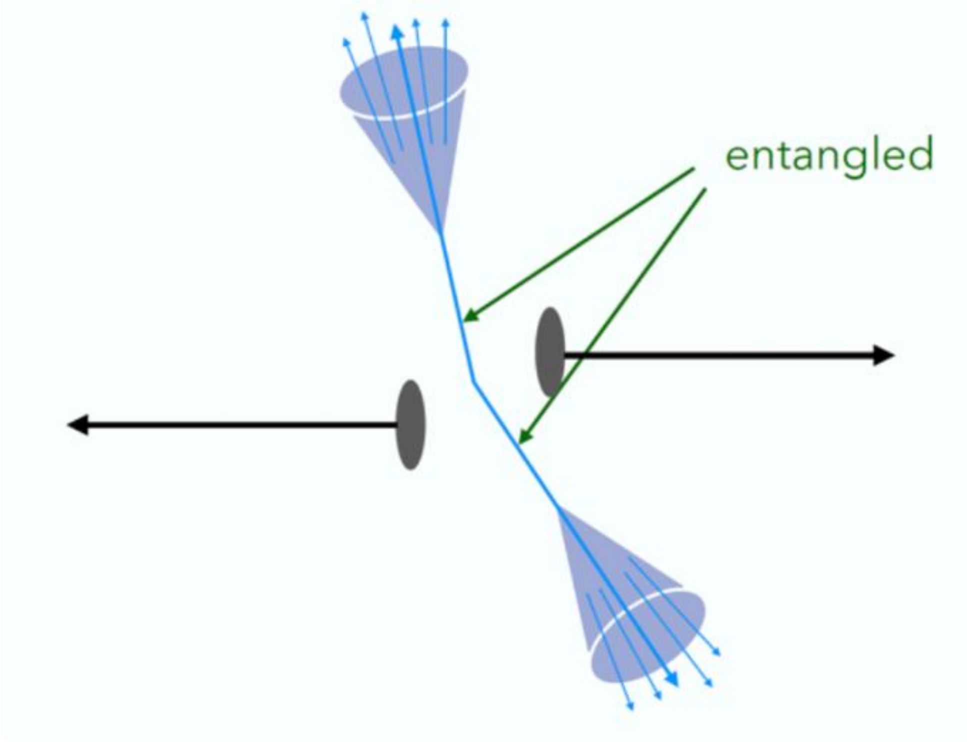

Originating in the same process, the partons possess quantum entanglement.

(Recent explorations of entanglement in DIS [Kharzeev, Levin '17], [Kharzeev '21])

Real-time quantum process requires

Real-time quantum simulation

Testbed for learning interesting physics with methods suitable for quantum simulation

Why Schwinger model?

- Simple enough for a first-principle real-time quantum simulation
- Has a lot of similarity with QCD in 3+1

Outline

- Schwinger model + jets

- Local operators and thermalization

- Entanglement, Schmidt states and hadronization

Schwinger model

Single-flavor (1+1)-dimensional QED:

$$\mathcal{L} = -\frac{1}{4}{F_{\mu\nu}}^2 + \bar{\psi}(i\gamma^\mu \partial_\mu - g\gamma^\mu A_\mu + m)\psi$$

Features include:

- No magnetic field/no dynamical photons
- Linear potential between "quarks" – confinement
- Chiral condensate (spontaneous chiral symmetry breaking at *m*=0)

Schwinger model

Single-flavor (1+1)-dimensional QED:

$$\mathcal{L} = -\frac{1}{4}{F_{\mu\nu}}^2 + \bar{\psi}(i\gamma^\mu\partial_\mu - g\gamma^\mu A_\mu + m)\psi$$

Features include:

- No magnetic field/no dynamical photons
- Linear potential between "quarks" – confinement
- Chiral condensate (spontaneous chiral symmetry breaking at *m*=0)

Massless case is exactly solvable, e.g. by bosonization:

$$\mathcal{L} = \frac{1}{2}(\partial_\mu\phi)^2 - \frac{1}{2}m_B^2\phi^2, \qquad m_B^2 = \frac{g^2}{\pi}$$

Schwinger model and jets: history

1974

Vacuum polarization and the absence of free quarks

A. Casher,* J. Kogut,† and Leonard Susskind‡

Massless Schwinger model with external source:

$$j_0^{\text{ext}} = g\delta(z-t), \quad j_1^{\text{ext}} = g\delta(z-t) \qquad \text{for } z>0,$$

$$j_0^{\text{ext}} = -g\delta(z+t), \quad j_1^{\text{ext}} = g\delta(z+t) \qquad \text{for } z<0,$$

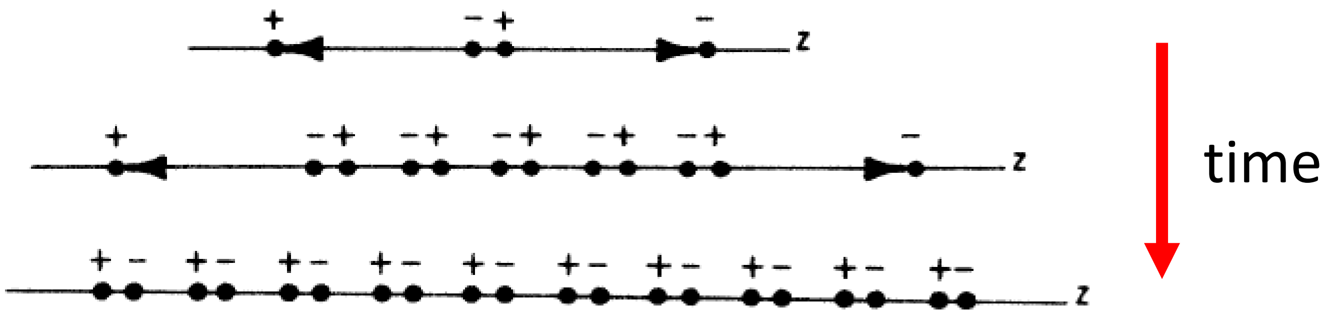

Schwinger model and jets: history

1974

Vacuum polarization and the absence of free quarks

A. Casher,* J. Kogut,† and Leonard Susskind‡

Massless Schwinger model with external source:

$$j_0^{\text{ext}} = g\delta(z-t), \quad j_1^{\text{ext}} = g\delta(z-t) \qquad \text{for } z>0,$$

$$j_0^{\text{ext}} = -g\delta(z+t), \quad j_1^{\text{ext}} = g\delta(z+t) \qquad \text{for } z<0,$$

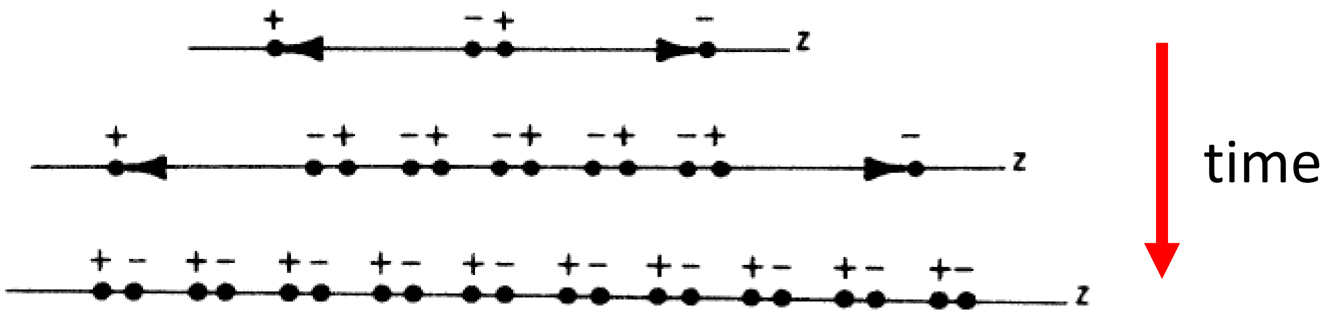

2012

Jet energy loss and fragmentation in heavy ion collisions

Dmitri E. Kharzeev[1,2] and Frashër Loshaj[1]

$$\phi(x) = \theta(t^2 - z^2)[1 - J_0(m\sqrt{t^2 - z^2})]$$

$$j^0 = \partial_z \phi$$

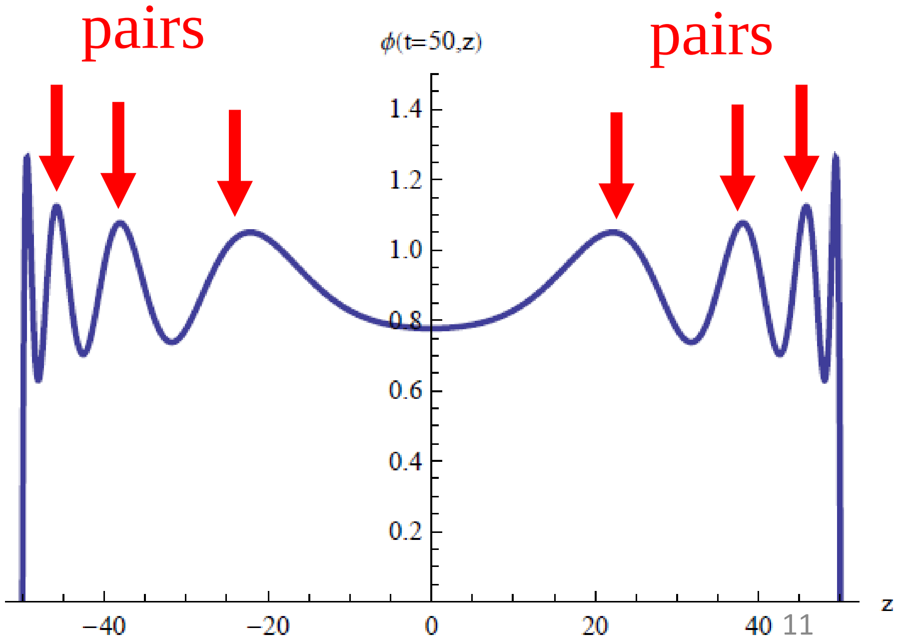

Schwinger model and jets: history

1974

Vacuum polarization and the absence of free quarks

A. Casher,* J. Kogut,† and Leonard Susskind‡

Massless Schwinger model with external source:

$j_0^{ext} = g\delta(z-t), \quad j_1^{ext} = g\delta(z-t) \qquad \text{for } z>0,$

$j_0^{ext} = -g\delta(z+t), \quad j_1^{ext} = g\delta(z$

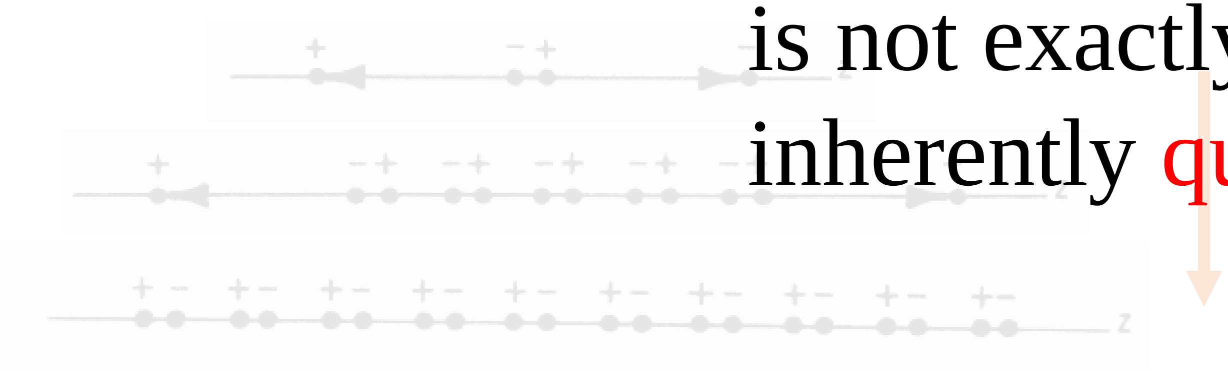

2012

Jet energy loss and fragmentation in heavy ion collisions

Dmitri E. Kharzeev[1,2] and Frashër Loshaj[1]

$\phi(x) = \theta(t^2 - z^2)[1 - J_0(m\sqrt{t^2 - z^2})]$

$j^0 = \partial_z \phi$

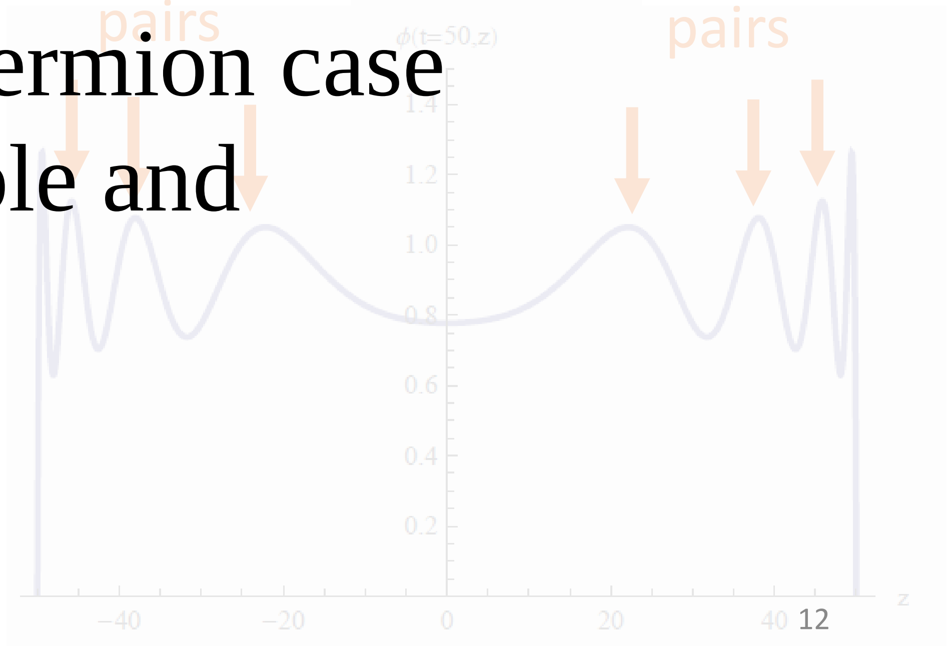

Classical treatment is mostly sufficient in the exactly solvable massless case

However, massive fermion case is not exactly solvable and inherently quantum

The massive Schwinger model on the lattice

Continuum: $$H = \int dx \left[\frac{1}{2}E^2 + \bar{\psi}(-i\gamma^1\partial_1 + g\gamma^1 A_1 + m)\psi\right]$$

Temporal gauge

$A_0 = 0$

The massive Schwinger model on the lattice

Continuum: $$H = \int dx \left[\frac{1}{2}E^2 + \bar{\psi}(-i\gamma^1\partial_1 + g\gamma^1 A_1 + m)\psi\right]$$

Temporal gauge
$A_0 = 0$

Fermion $\psi(a\,n)$ $\Rightarrow$ $$\frac{1}{\sqrt{a}}\begin{pmatrix}\chi_{2n}\\ \chi_{2n-1}\end{pmatrix}$$ Kogut-Susskind

$$\{\psi_a(x), \psi_b^\dagger(y)\} = \delta_{ab}\delta(x-y) \quad \Rightarrow \quad \{\chi_i, \chi_j^\dagger\} = \delta_{ij}$$

N sites encode
N/2 physical sites

The massive Schwinger model on the lattice

Continuum: $$H = \int dx \left[\frac{1}{2}E^2 + \bar{\psi}(-i\gamma^1\partial_1 + g\gamma^1 A_1 + m)\psi\right]$$

Temporal gauge
$A_0 = 0$

Fermion $\psi(a\,n) \Rightarrow \frac{1}{\sqrt{a}}\begin{pmatrix}\chi_{2n}\\ \chi_{2n-1}\end{pmatrix}$ Kogut-Susskind

$\{\psi_a(x), \psi_b^\dagger(y)\} = \delta_{ab}\delta(x-y) \Rightarrow \{\chi_i, \chi_j^\dagger\} = \delta_{ij}$

N sites encode
N/2 physical sites

Gauge field $E(x = a\,n) \Rightarrow L_n$

Gauss law $\partial_1 E - g j^0 = 0 \Rightarrow L_n - L_{n-1} - q_n = 0, \quad q_i = \chi_i^\dagger \chi_i + \frac{(-1)^i - 1}{2}$

With open boundary conditions the electric field is fully determined by the fermions

Mapping to a spin chain (optional)

X, Y, Z – Pauli matrices

$$X_n \equiv \underset{1^{\mathrm{st}}}{I} \otimes \cdots \otimes \underset{(n-1)^{\mathrm{th}}}{I} \otimes \underset{n^{\mathrm{th}}}{X} \otimes \underset{(n+1)^{\mathrm{th}}}{I} \otimes \cdots \otimes I \quad \text{etc.}$$

Mapping to a spin chain (optional)

X, Y, Z – Pauli matrices

$$\chi_n = \frac{X_n - iY_n}{2}\prod_{j=1}^{n-1}(-iZ_j),$$

$$\chi_n^\dagger = \frac{X_n + iY_n}{2}\prod_{j=1}^{n-1}(iZ_j),$$

$$X_n \equiv \underset{1^{\text{st}}}{I} \otimes \cdots \otimes \underset{(n-1)^{\text{th}}}{I} \otimes \underset{n^{\text{th}}}{X} \otimes \underset{(n+1)^{\text{th}}}{I} \otimes \cdots \otimes I$$ etc.

Jordan-Wigner transformation

Mapping to a spin chain (optional)

X, Y, Z – Pauli matrices

$$X_n \equiv \underset{1^{\text{st}}}{I} \otimes \cdots \otimes \underset{(n-1)^{\text{th}}}{I} \otimes \underset{n^{\text{th}}}{X} \otimes \underset{(n+1)^{\text{th}}}{I} \otimes \cdots \otimes I$$ etc.

$$\chi_n = \frac{X_n - iY_n}{2} \prod_{j=1}^{n-1} (-iZ_j),$$

$$\chi_n^\dagger = \frac{X_n + iY_n}{2} \prod_{j=1}^{n-1} (iZ_j),$$

Jordan-Wigner transformation

Spin chain Hamiltonian:

$$H^L = \underbrace{\frac{1}{4a} \sum_{n=1}^{N-1} (X_n X_{n+1} + Y_n Y_{n+1})}_{\text{Kinetic term}} + \underbrace{\frac{m}{2} \sum_{n=1}^{N} (-1)^n Z_n}_{\text{Mass term}} + \underbrace{\frac{ag^2}{2} \sum_{n=1}^{N-1} L_n^2}_{\text{Nonlocal electric field term}}$$

$$L_n = \sum_{i=1}^{n} q_i$$

$$q_{n,t} = \frac{\langle Z_n \rangle_t + (-1)^n}{2a}$$

Adding the jets

$$j^0_{\text{ext}}(x,t) = g[\delta(\Delta x - \Delta t) - \delta(\Delta x + \Delta t)]\theta(\Delta t)$$

$$j^1_{\text{ext}}(x,t) = g[\delta(\Delta x - \Delta t) + \delta(\Delta x + \Delta t)]\theta(\Delta t)$$

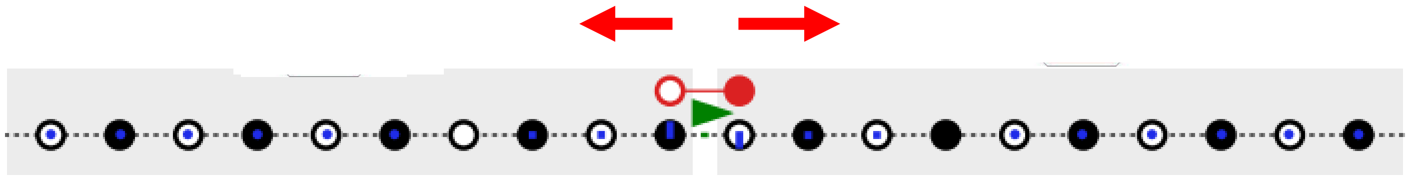

$$H = \int dx \left[\bar{\psi}(-i\gamma^1\partial_1 + g\gamma^1 A_1 + m)\psi + \frac{1}{2}E^2 + j^1_{\text{ext}}(x,t)A_1 \right]$$

$$H^L(t) = \frac{1}{4a}\sum_{n=1}^{N-1}(X_n X_{n+1} + Y_n Y_{n+1}) + \frac{m}{2}\sum_{n=1}^{N}(-1)^n Z_n + \frac{ag^2}{2}\sum_{n=1}^{N-1}(L_{\text{dyn},n} + L_{\text{ext},n}(t))^2.$$

$$L_{\text{dyn},n} = \sum_{i=1}^{n} q_i$$

$$L_{\text{ext},n}(t) = -\theta\left(t - t_0 - \left|x - x_0 + \frac{a}{2}\right|\right)$$

Numerical procedure

Start from the ground state of the Hamiltonian:

$$H(t=0)|\Psi(t=0)\rangle = E_0|\Psi(t=0)\rangle$$

Switch on the external source and time evolve:

$$|\Psi_t\rangle = \mathcal{T}e^{-i\int_0^t dt' H(t')}|\Psi_0\rangle$$

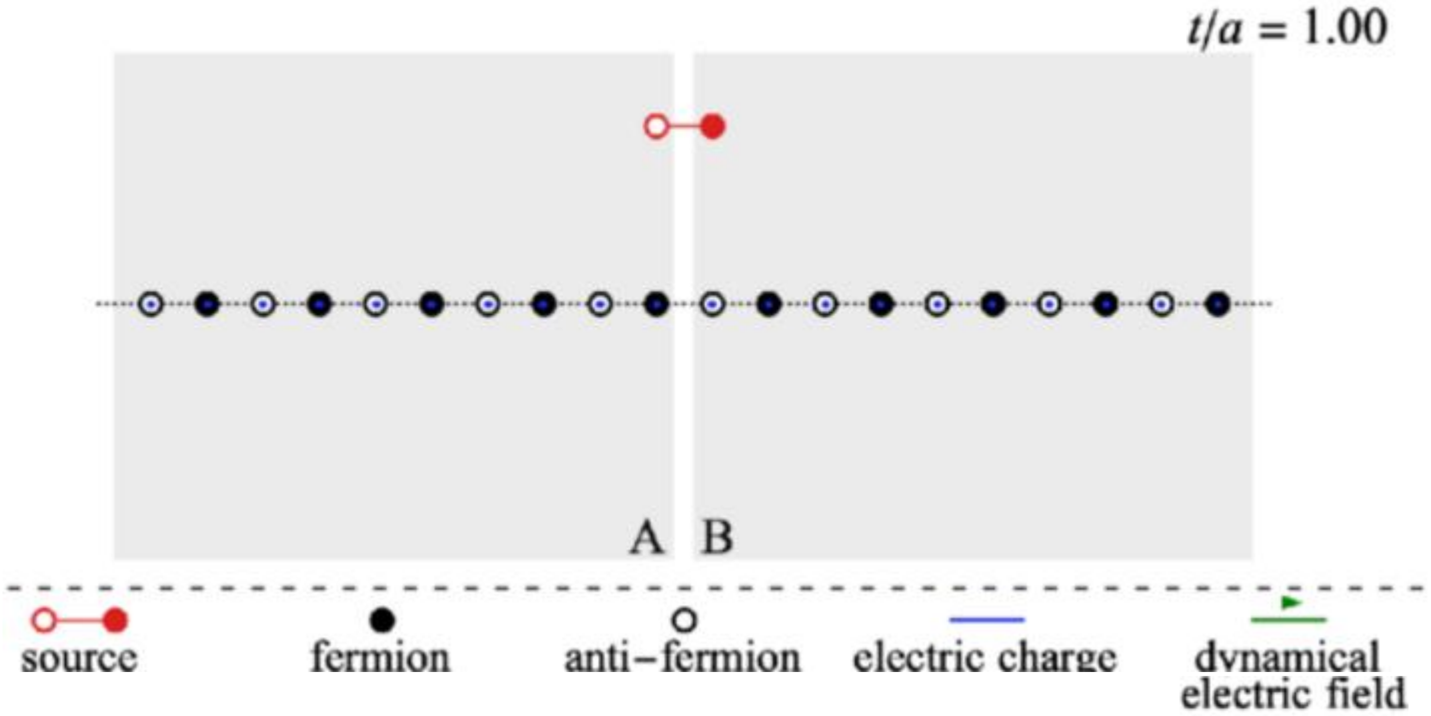

Numerical time evolution using classical exact diagonalization or tensor networks mimics simulation on a quantum device

Screening, chiral condensate and entanglement

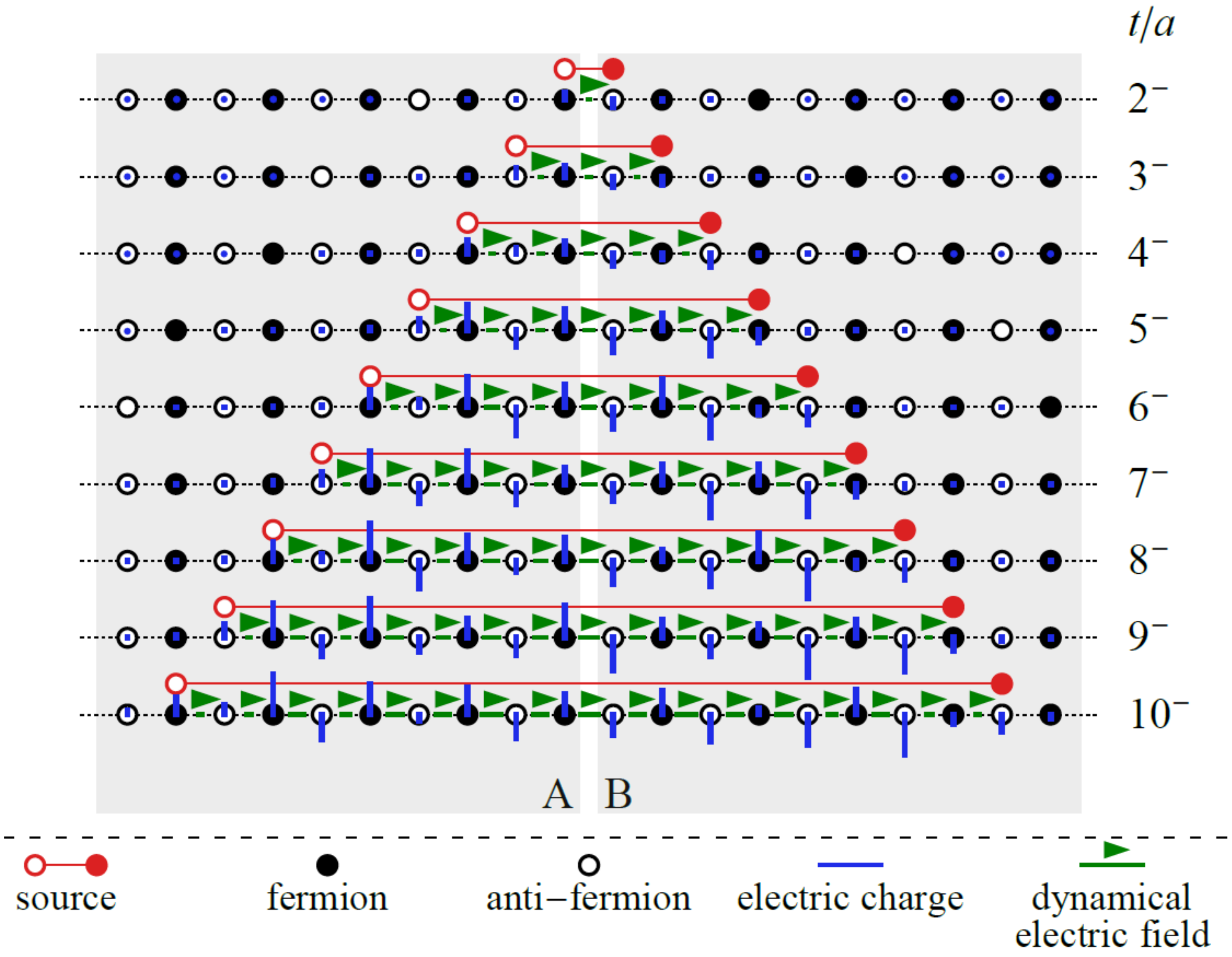

$$q_{n,t} = \langle \psi^\dagger(an)\psi(an)\rangle_t = \frac{\langle Z_n\rangle_t + (-1)^n}{2a}$$

$$L_n = L_{\text{dyn},n} + L_{\text{ext},n}(t)$$

$$L_{\text{dyn},n} = \sum_{i=1}^{n} q_i$$

$$L_{\text{ext},n}(t) = -\theta\left(\frac{t-t_0}{a} - \left|n - \frac{N}{2}\right|\right)$$

$$\nu_{n,t} = \langle \bar{\psi}(an)\psi(an)\rangle_t = \frac{(-1)^n\langle Z_n\rangle_t}{2a}$$

Screening, chiral condensate and entanglement

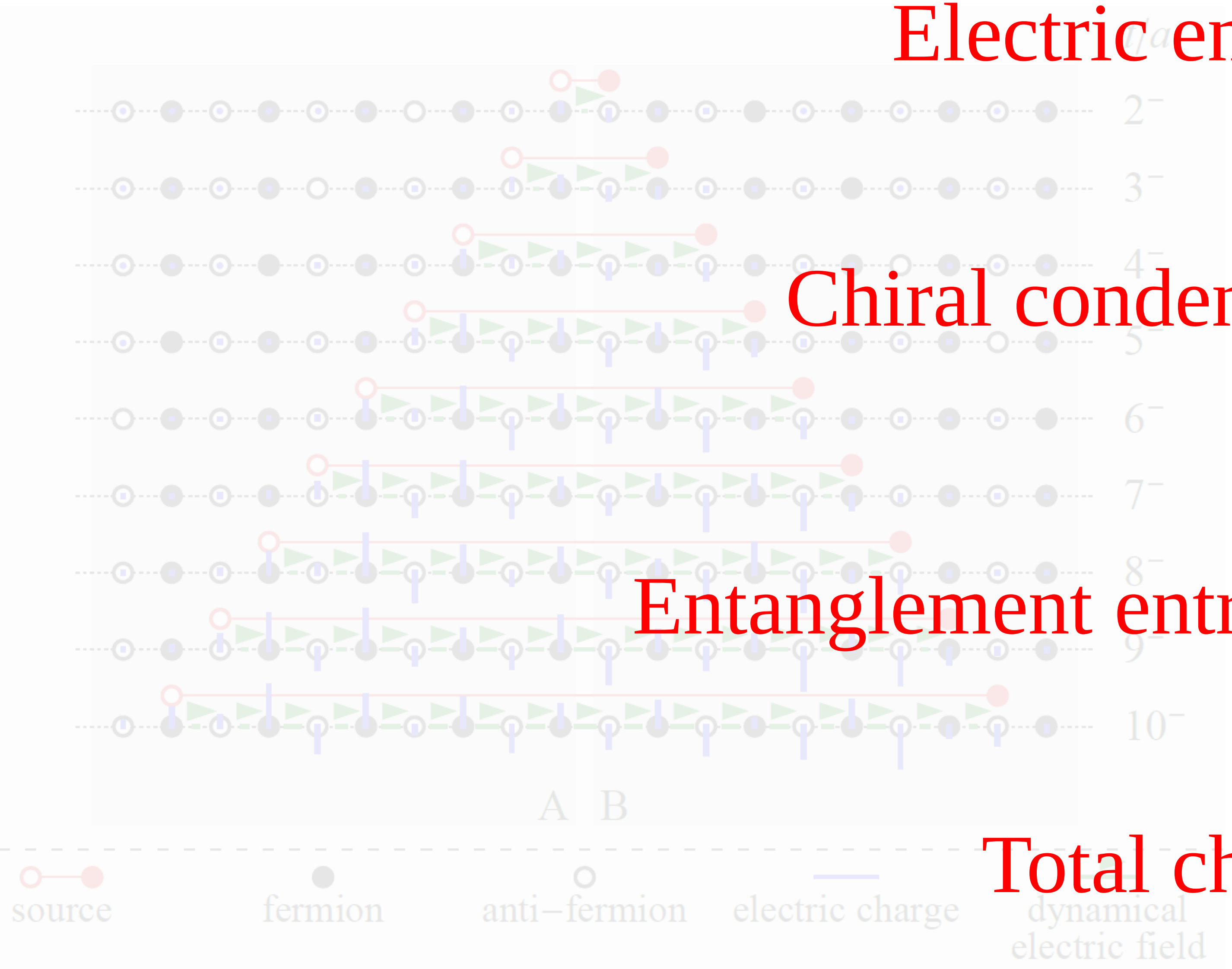

Electric energy

Chiral condensate

Entanglement entropy

Total charge

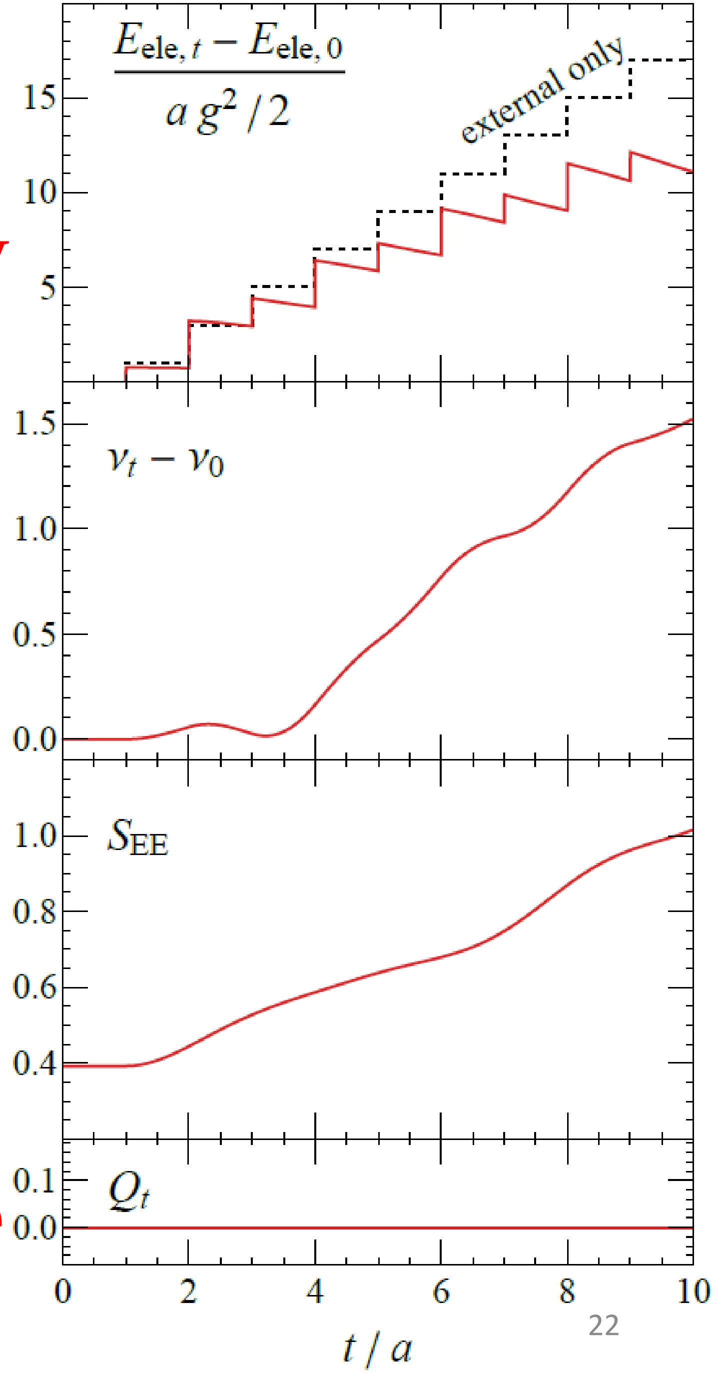

Screening, chiral condensate and entanglement

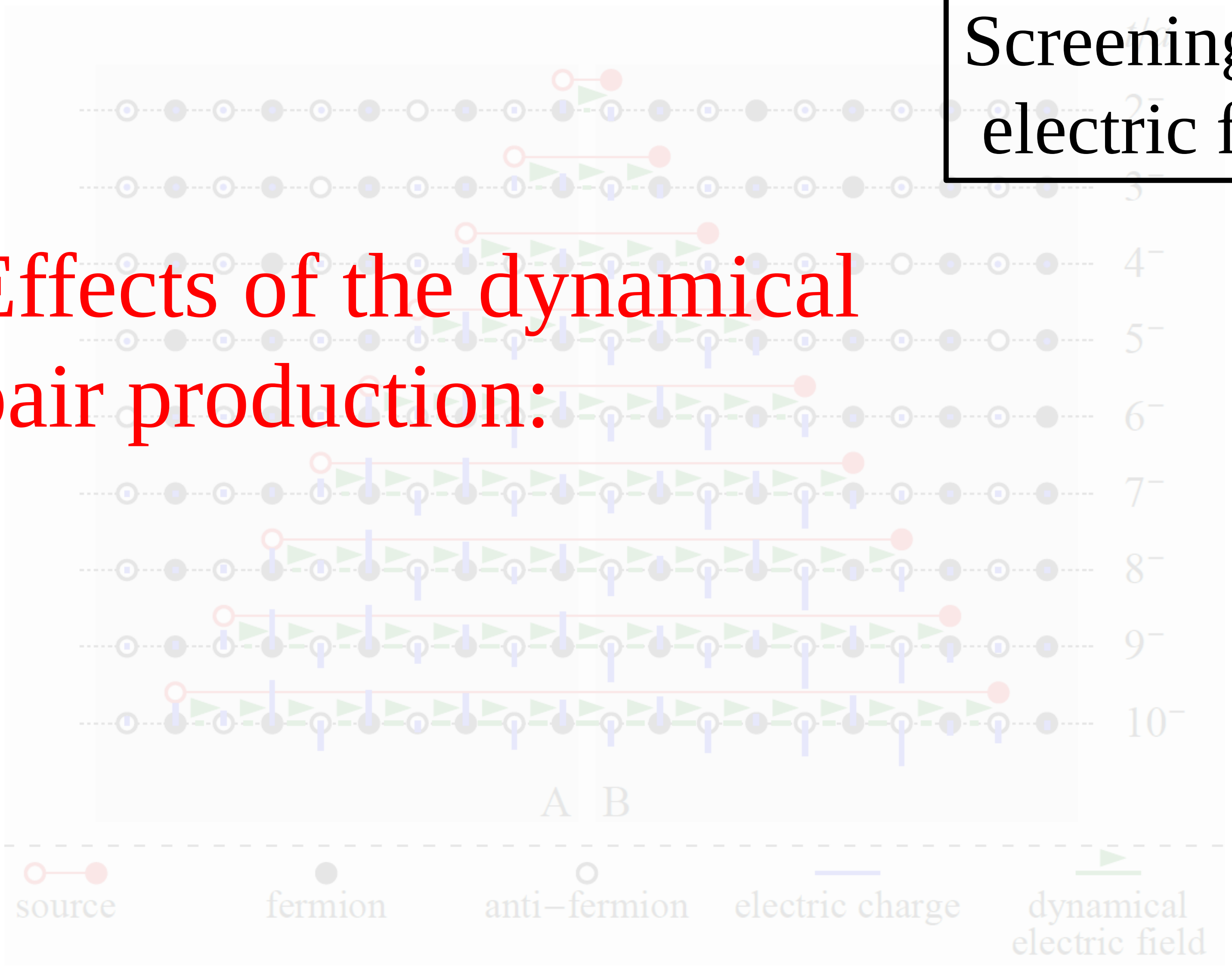

Screening the electric field

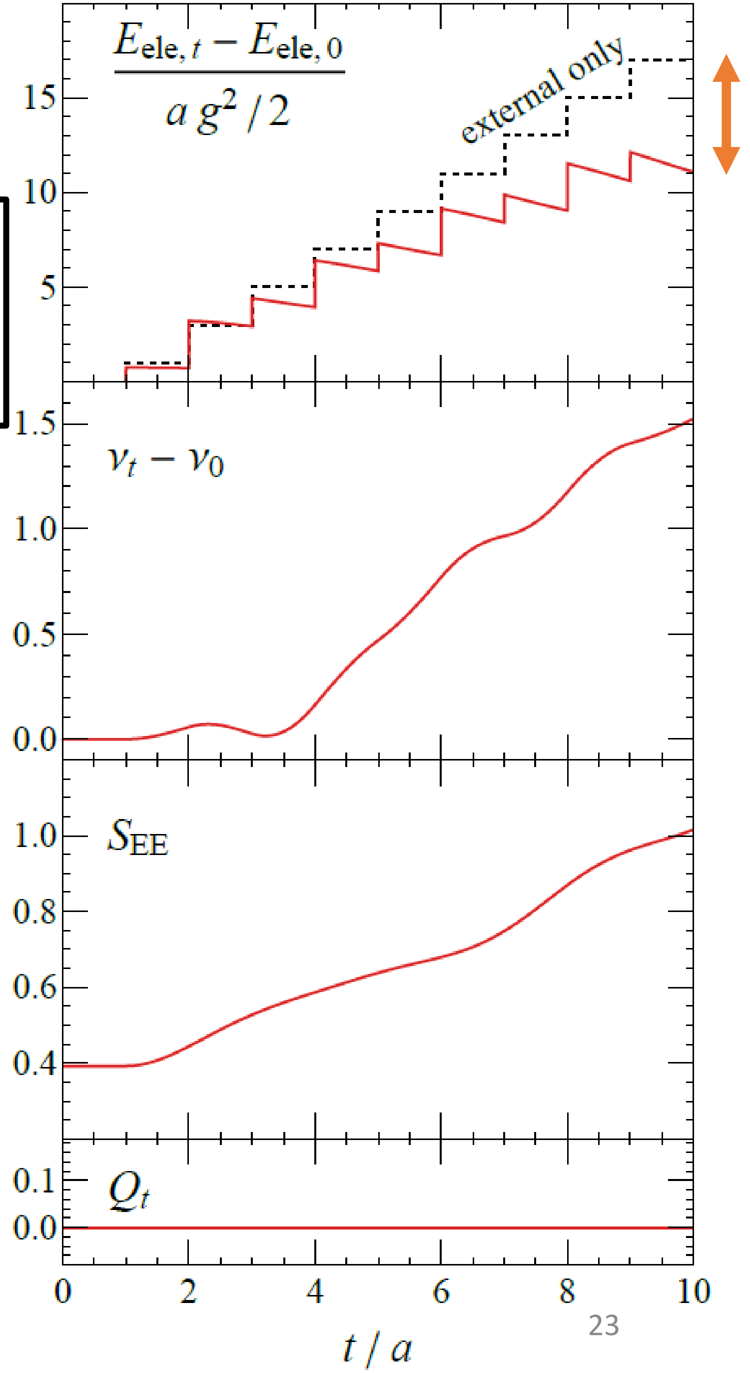

Effects of the dynamical pair production:

Screening, chiral condensate and entanglement

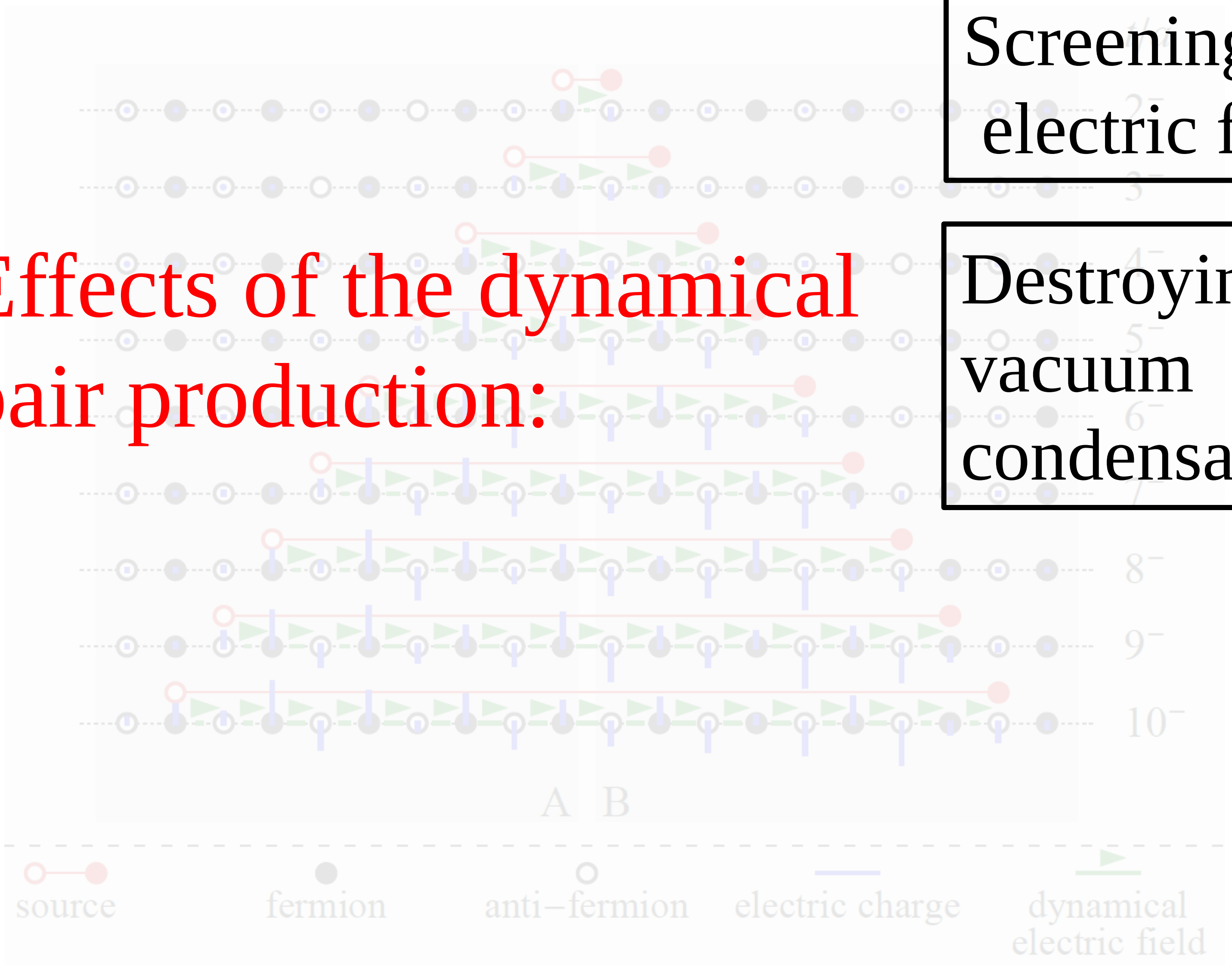

Effects of the dynamical pair production:

Screening the electric field

Destroying vacuum condensate

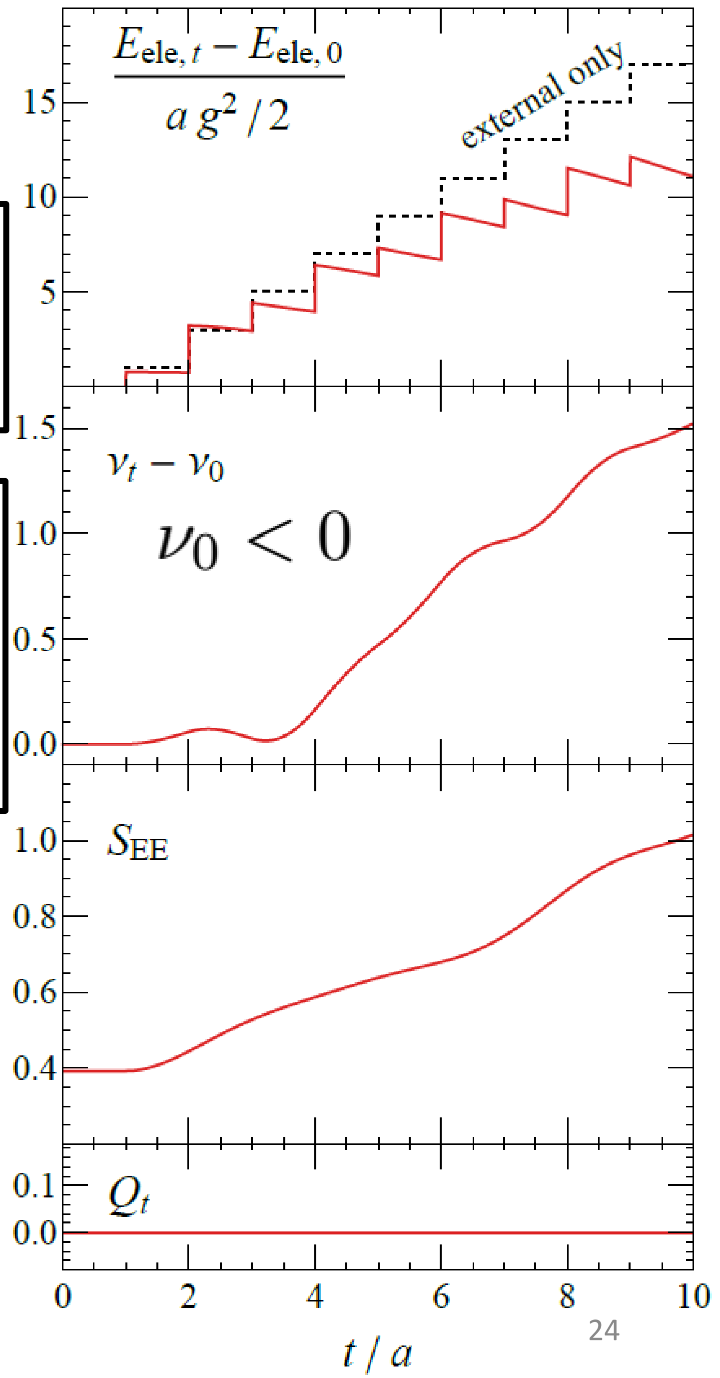

Screening, chiral condensate and entanglement

Effects of the dynamical pair production:

$$\rho_A = \mathrm{Tr}_B \rho, \qquad S_{EE} = -\mathrm{Tr}_A(\rho_A \log \rho_A)$$

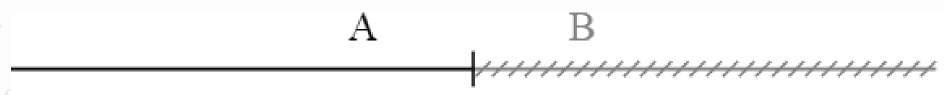

Screening the electric field

Destroying vacuum condensate

Entangling the jets

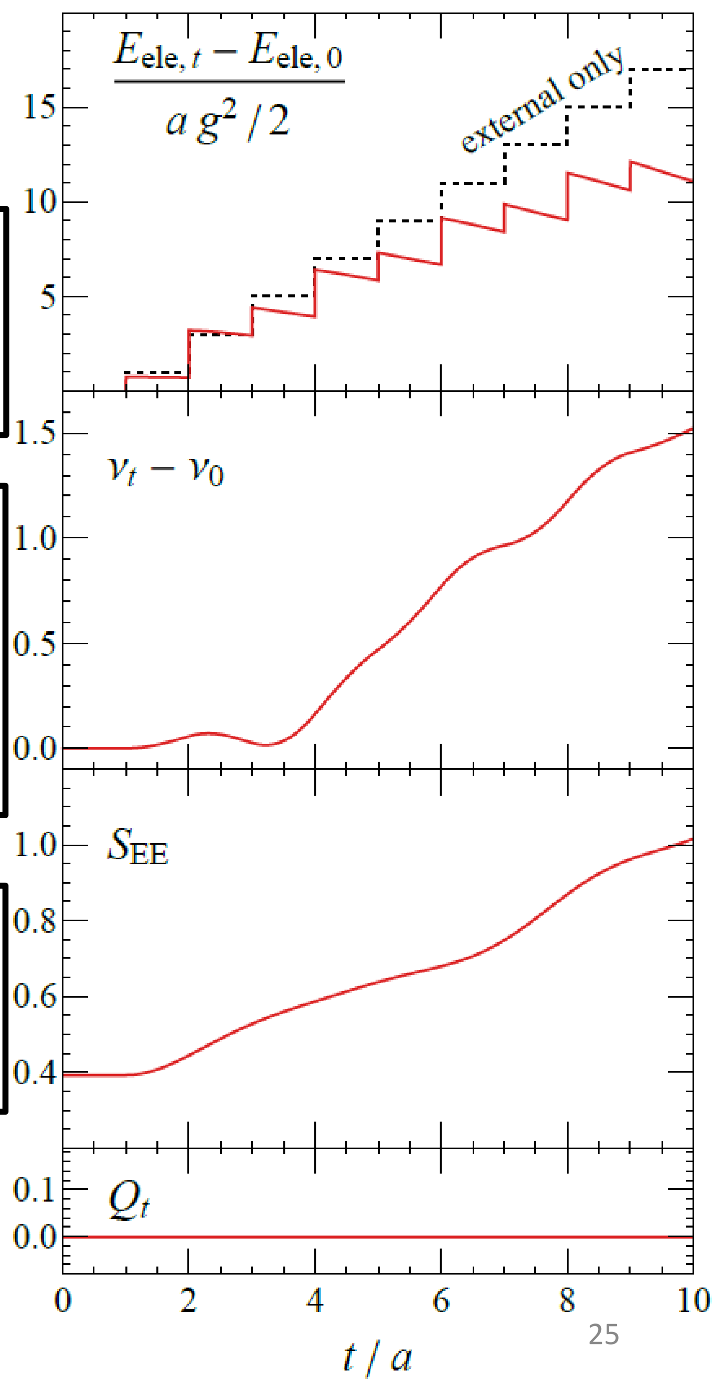

Towards thermalization

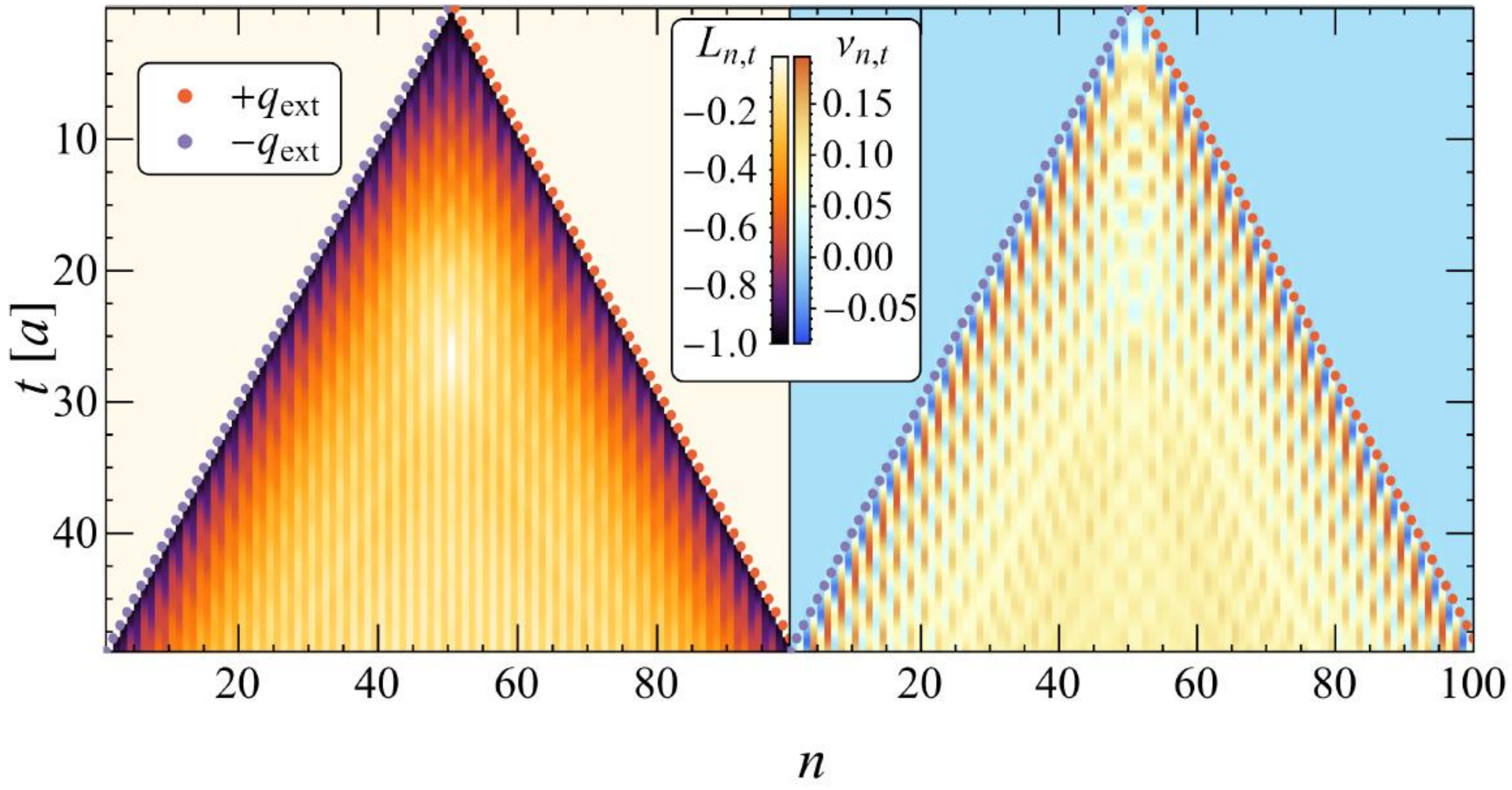

Towards thermalization

Compare to exact diagonalization

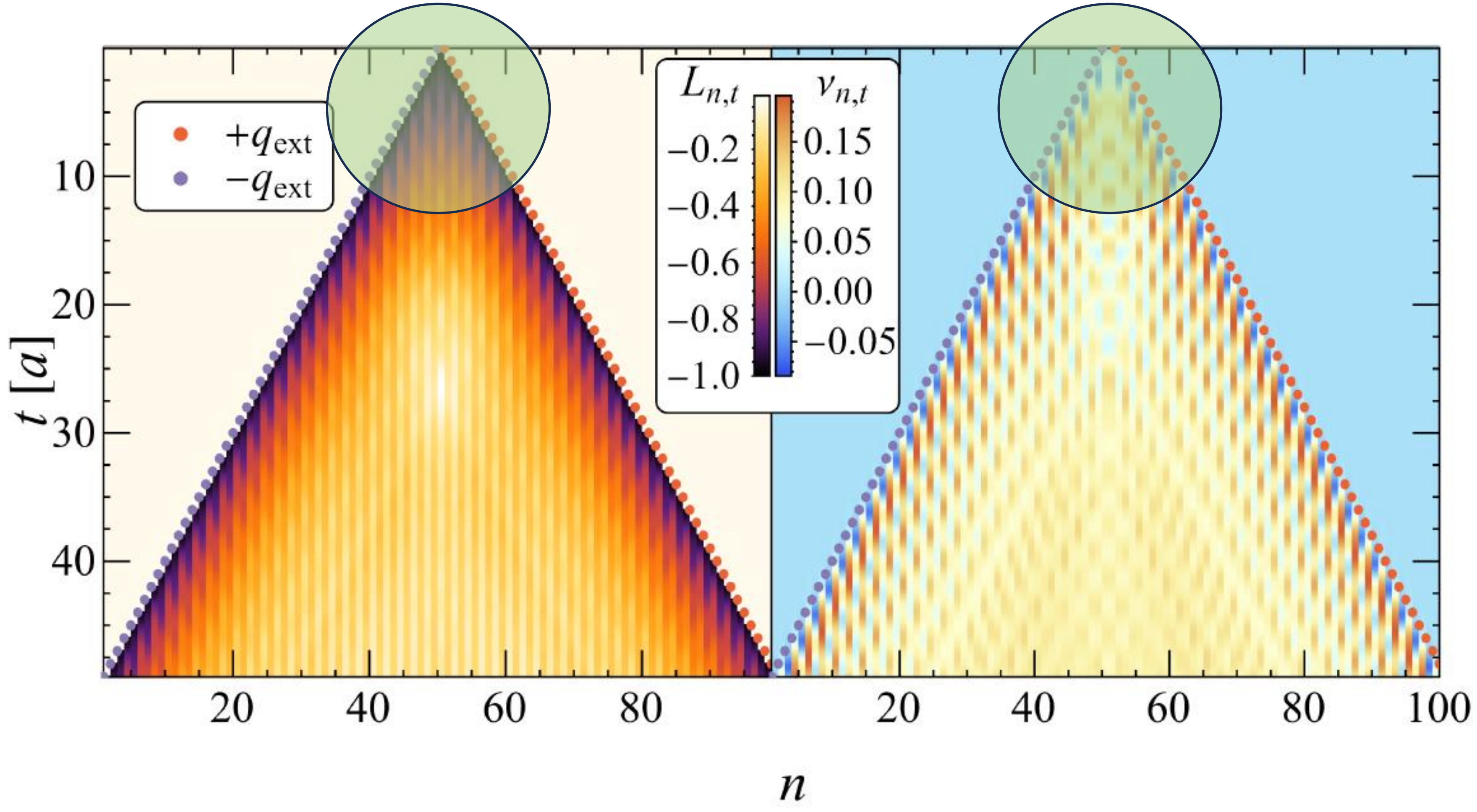

Tensor network methods allow studying much larger system

Towards thermalization

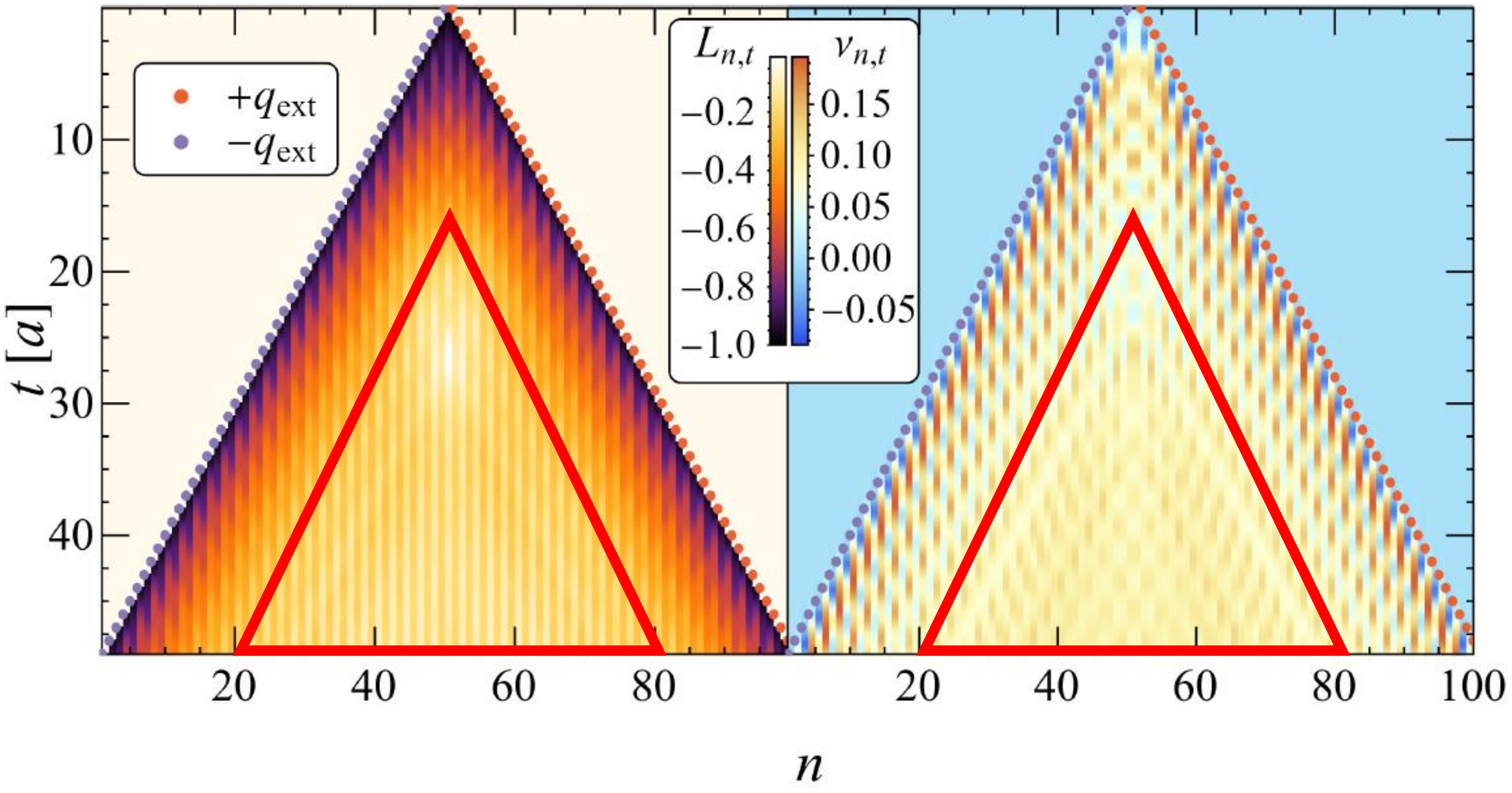

Equilibration towards late times

Towards thermalization

Averaging over the central part

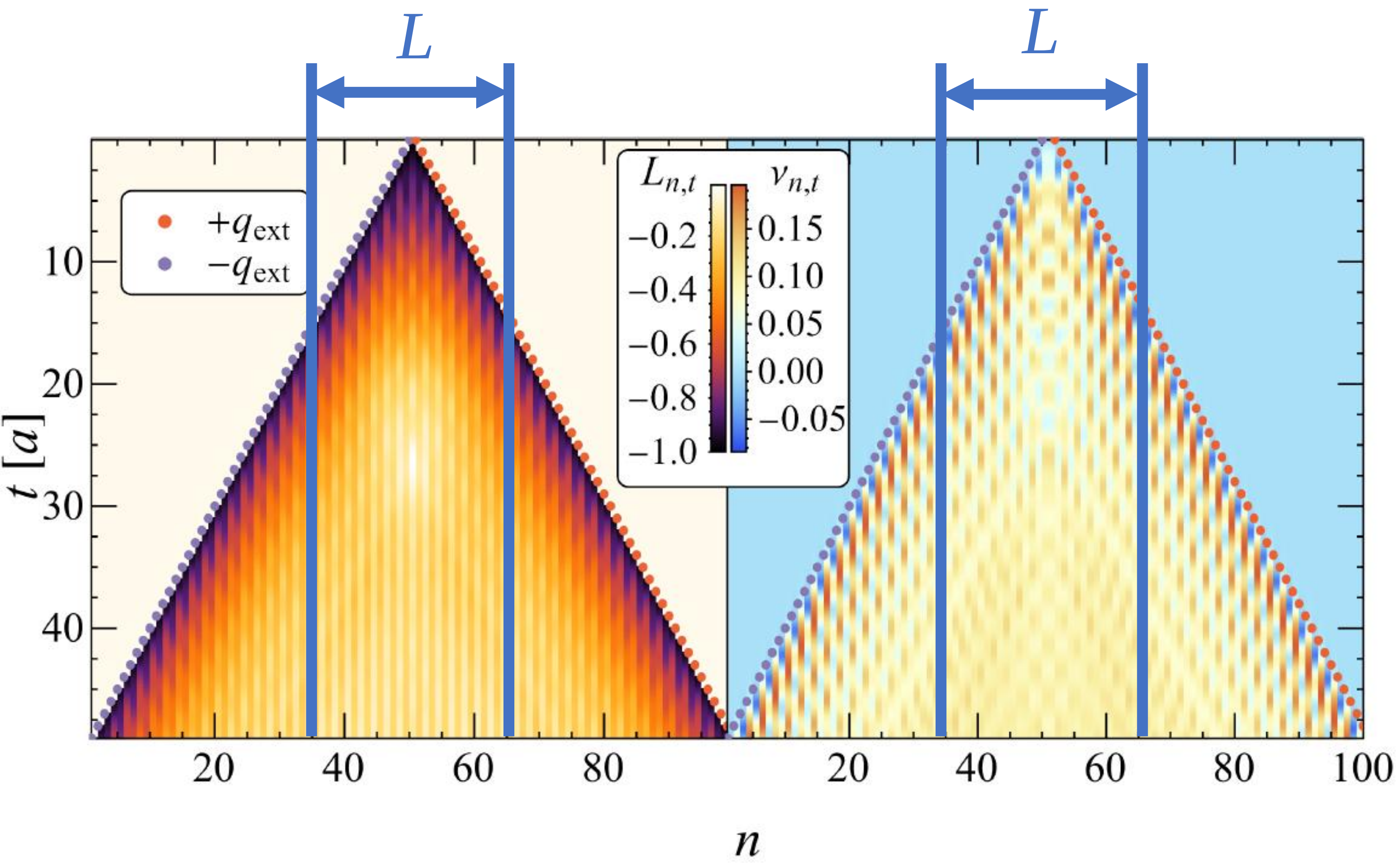

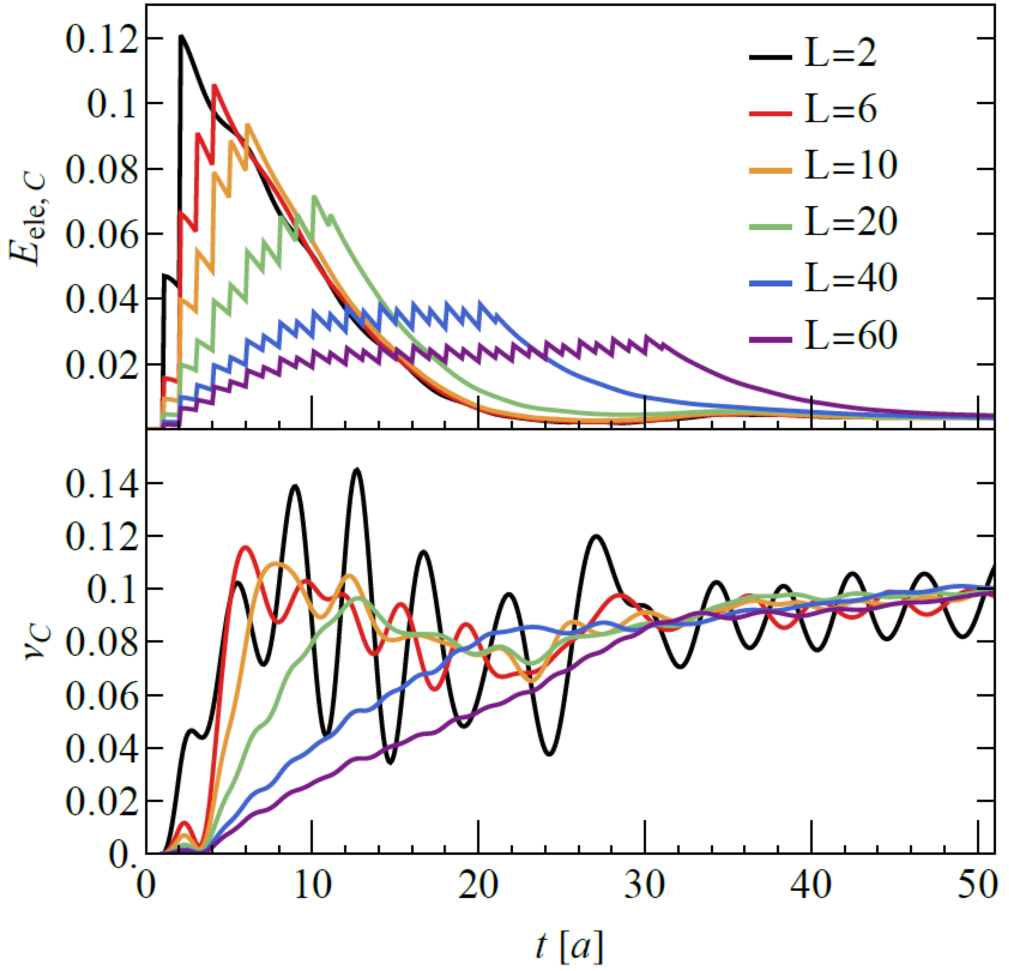

Equilibration towards late times

Thermal expectation values

For any operator

$$\langle \mathcal{O} \rangle_T = \frac{\sum_n e^{-E_n/T} \langle E_n | \mathcal{O} | E_n \rangle}{\sum_n e^{-E_n/T}}$$

where

$$H|E_n\rangle = E_n|E_n\rangle$$

Access the whole spectrum with exact diagonalization

Can also access Gibbs entropy:

$$S = -\sum_n p_n \log p_n \,, \quad p_n = e^{-E_n/T}$$

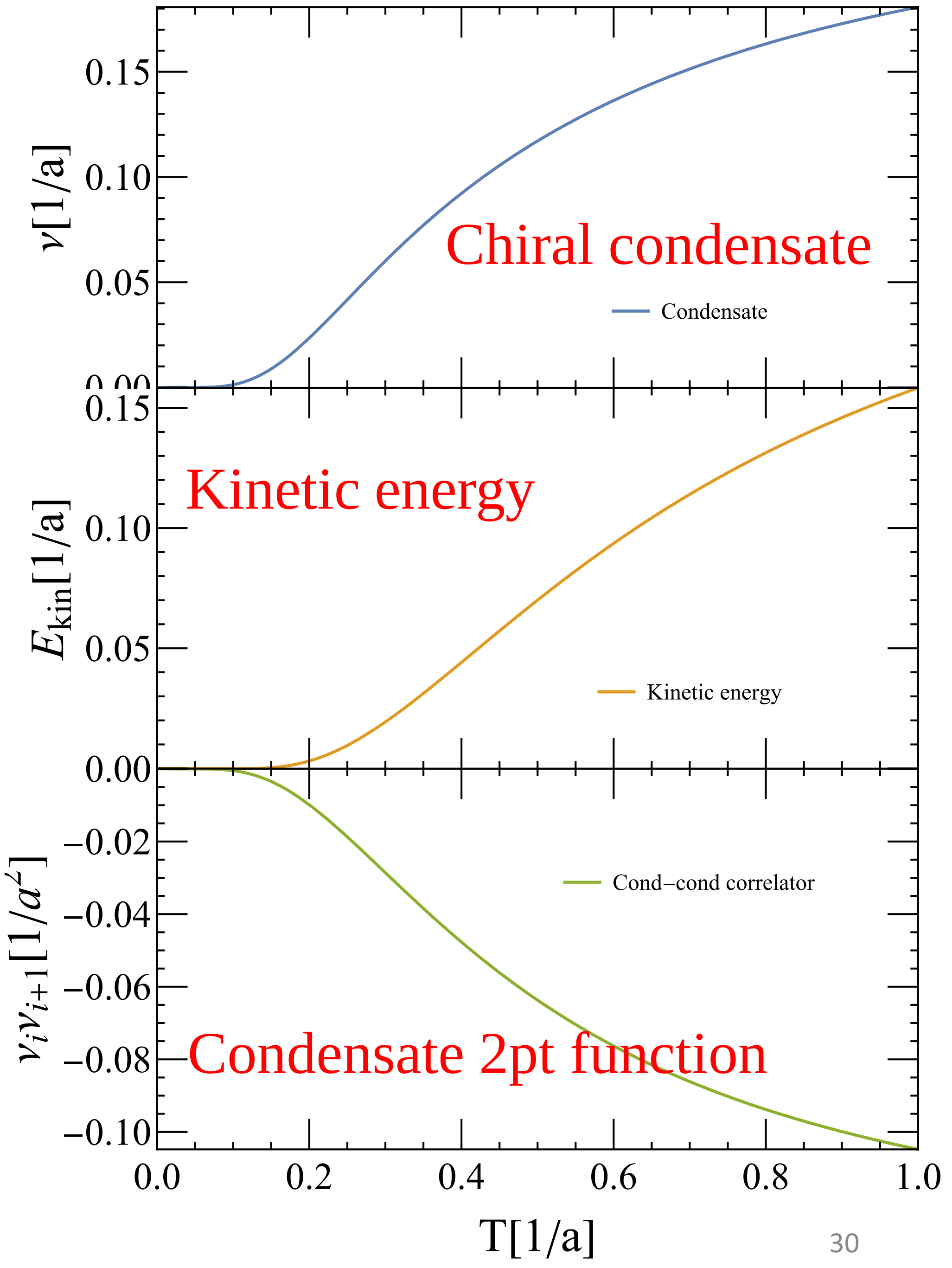

Thermalization dynamics

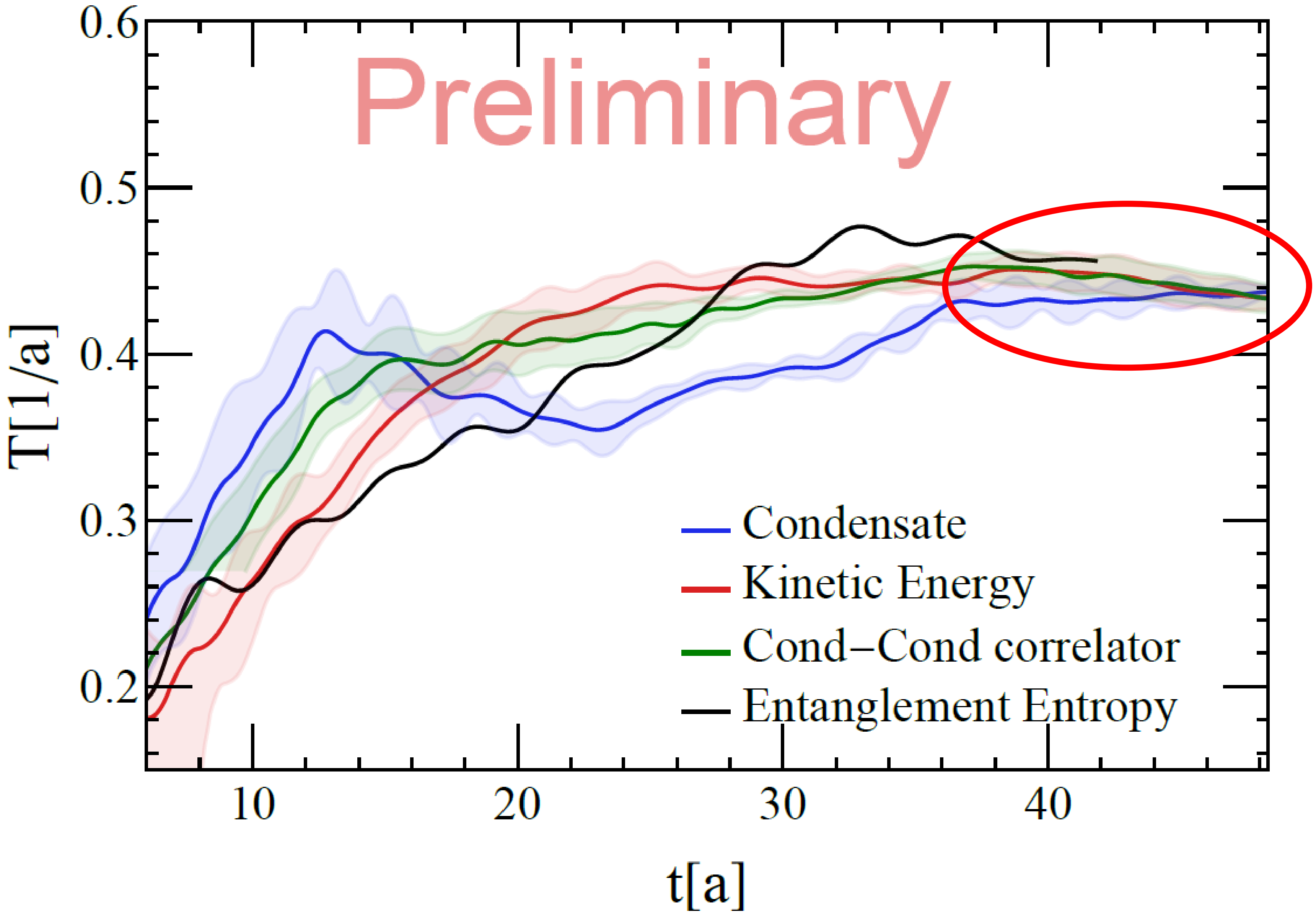

Reaching a universal temperature

Renyi entropy of the central region

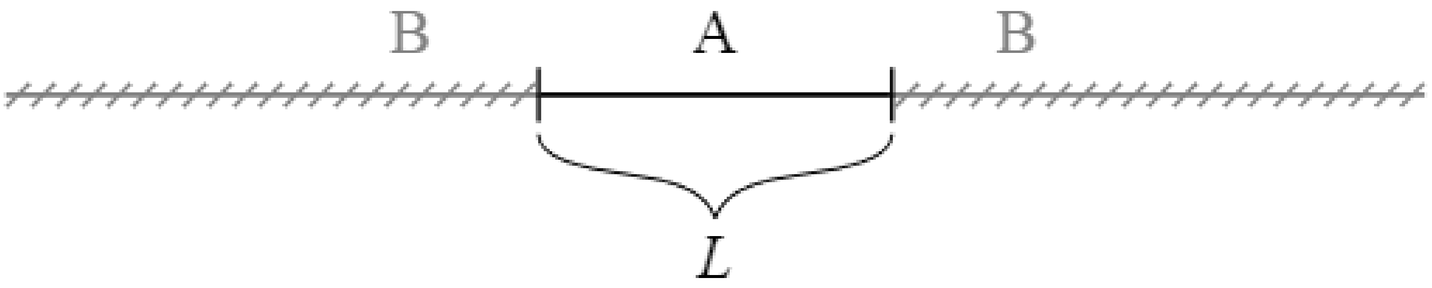

$$S_2(L) = -\log \mathrm{Tr}(\rho_A^2)$$

Study as a function of L

Ground state: “area law” (L-independent)

Typical state, e.g. thermal: “volume law” (linear in L)

E. Bianchi, L. Hackl, M. Kieburg, M. Rigol, and L. Vidmar,
PRX Quantum **3** (2022)

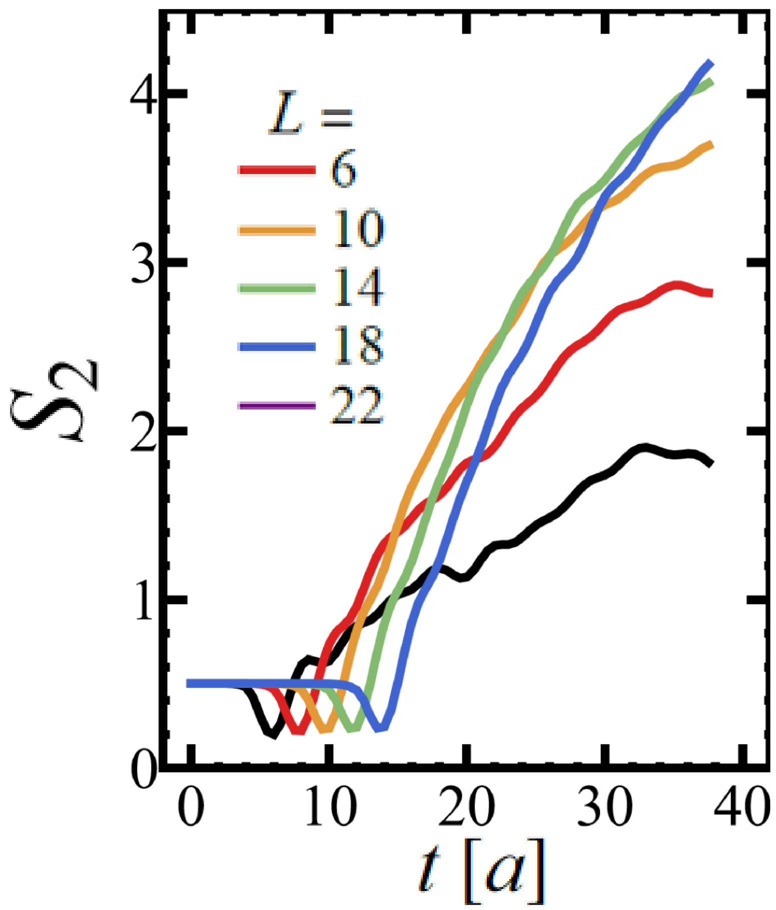

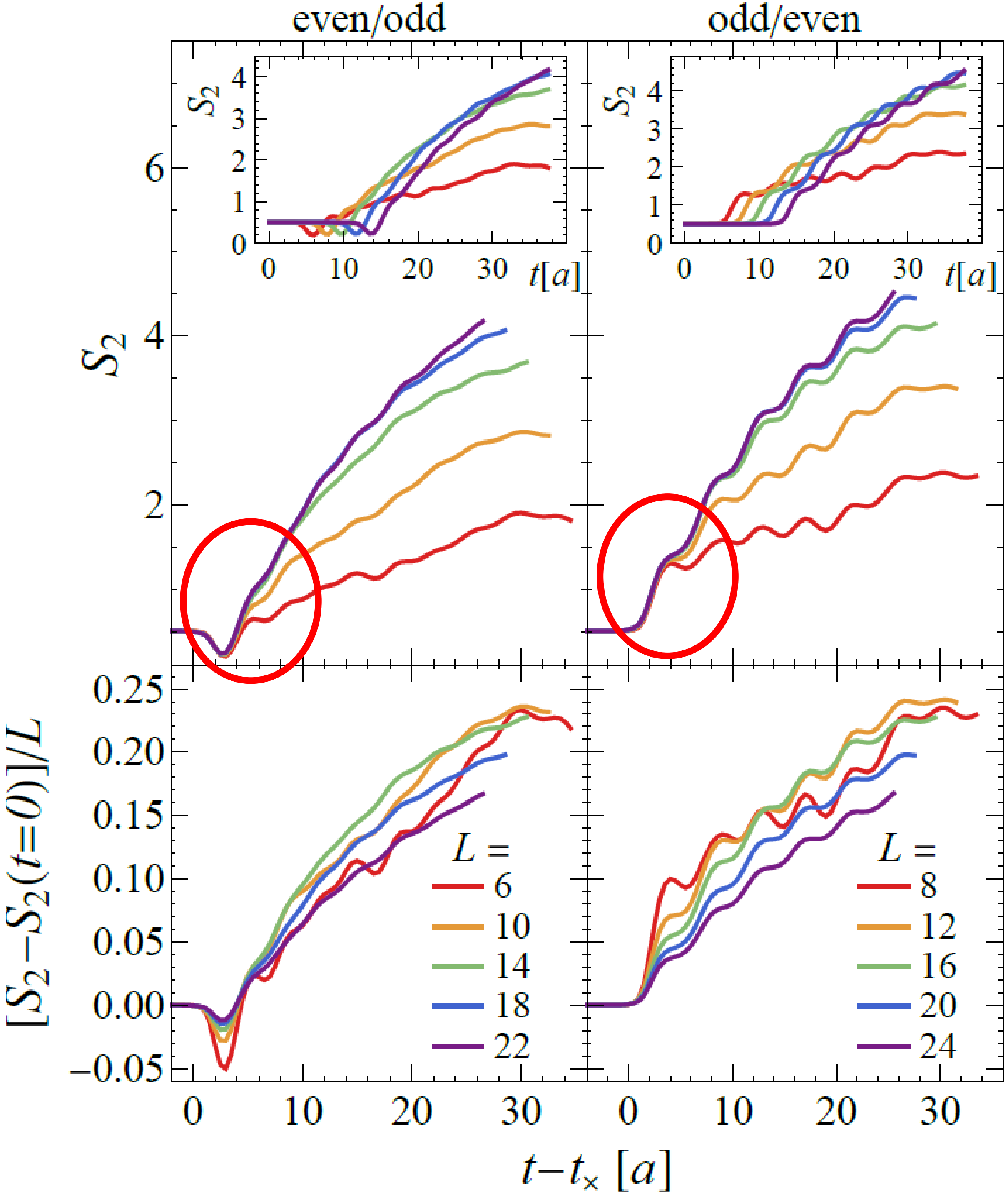

Area and volume laws of entanglement

Adjust by the jet arrival time

area law at early times

Area and volume laws of entanglement

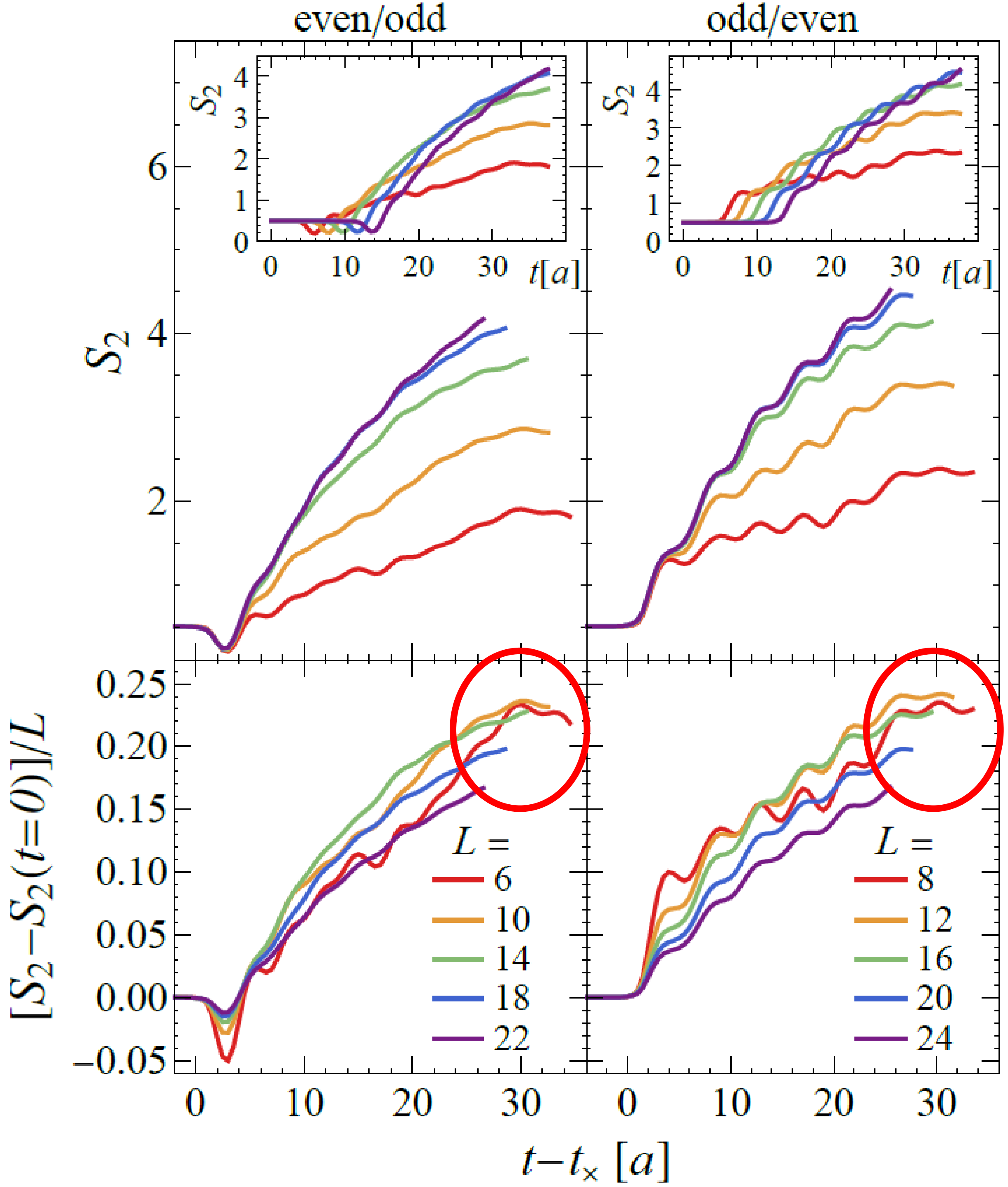

Adjust by the jet arrival time

area law at early times

Rescale by the subsystem size

volume law at late times

Entanglement spectrum

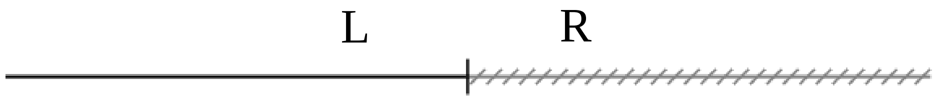

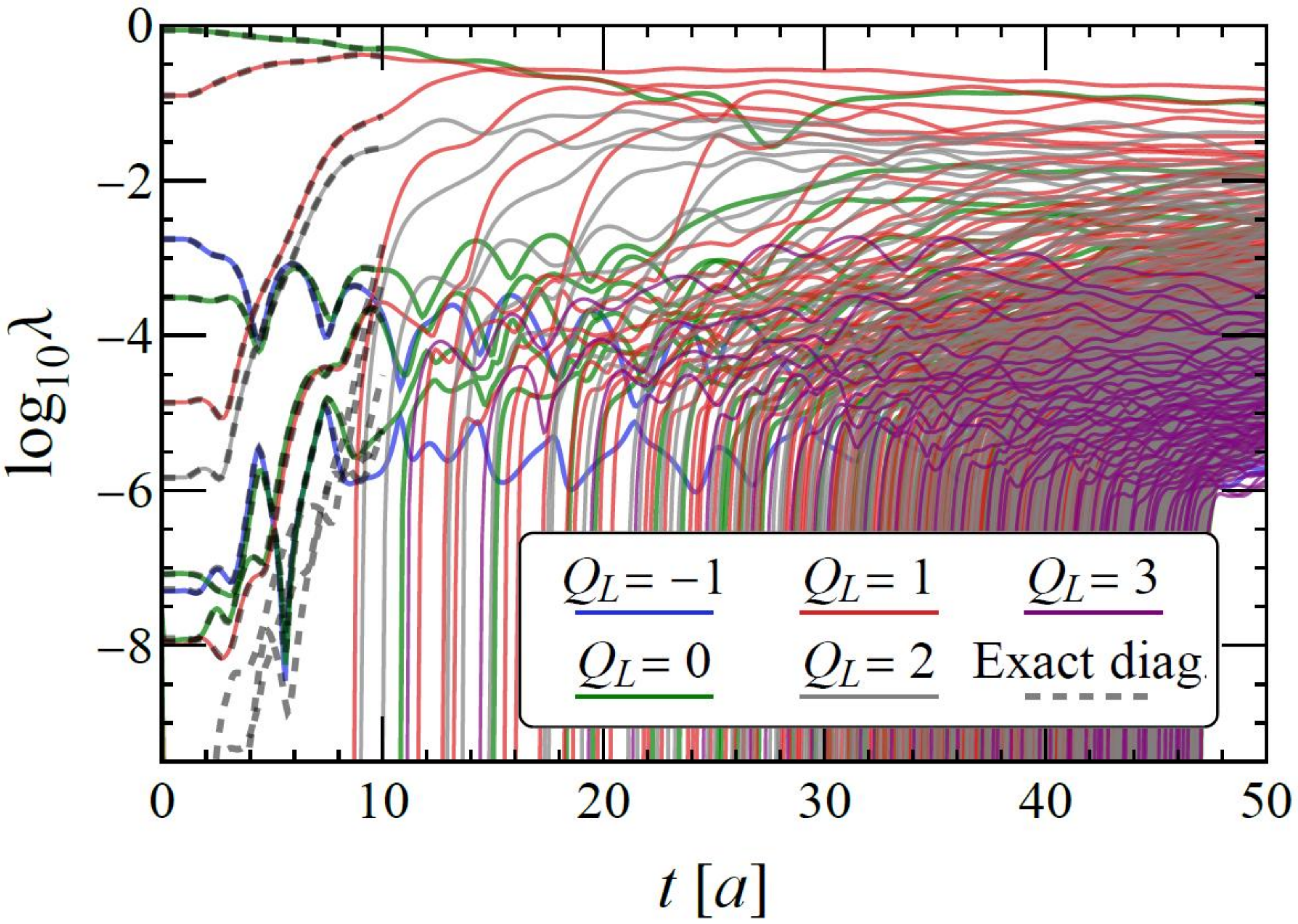

Schmidt decomposition:

$$|\Psi(t)\rangle = \sum_{i=1}^{2^{N/2}} \sqrt{\lambda_i(t)}|\psi_i^L(t)\rangle \otimes |\psi_i^R(t)\rangle$$

$$\rho_L(t) = \sum_{i=1}^{2^{N/2}} \lambda_i(t)|\psi_i^L(t)\rangle\langle\psi_i^L(t)|$$

$$S_{EE}(t) = -\sum_{i=1}^{2^{N/2}} \lambda_i \ln \lambda_i$$

Symmetry-resolved:

$$\sum_{n=1}^{N/2} q_n|\psi_i^L\rangle \equiv Q_L|\psi_i^L\rangle$$

Renyi entropies and entangleness

$$S_\alpha(t) \equiv \frac{\ln \mathrm{Tr}_L(\rho_L(t)^\alpha)}{1-\alpha} = \frac{\ln \sum_{i=1}^{2^{N/2}} \lambda_i^\alpha}{1-\alpha}$$

$$\mathcal{E} \equiv \frac{1-\mathrm{tr}\rho_L^2}{1-2^{-N/2}} = \frac{1-\sum_{i=1}^{2^{N/2}} \lambda^2}{1-2^{-N/2}}$$

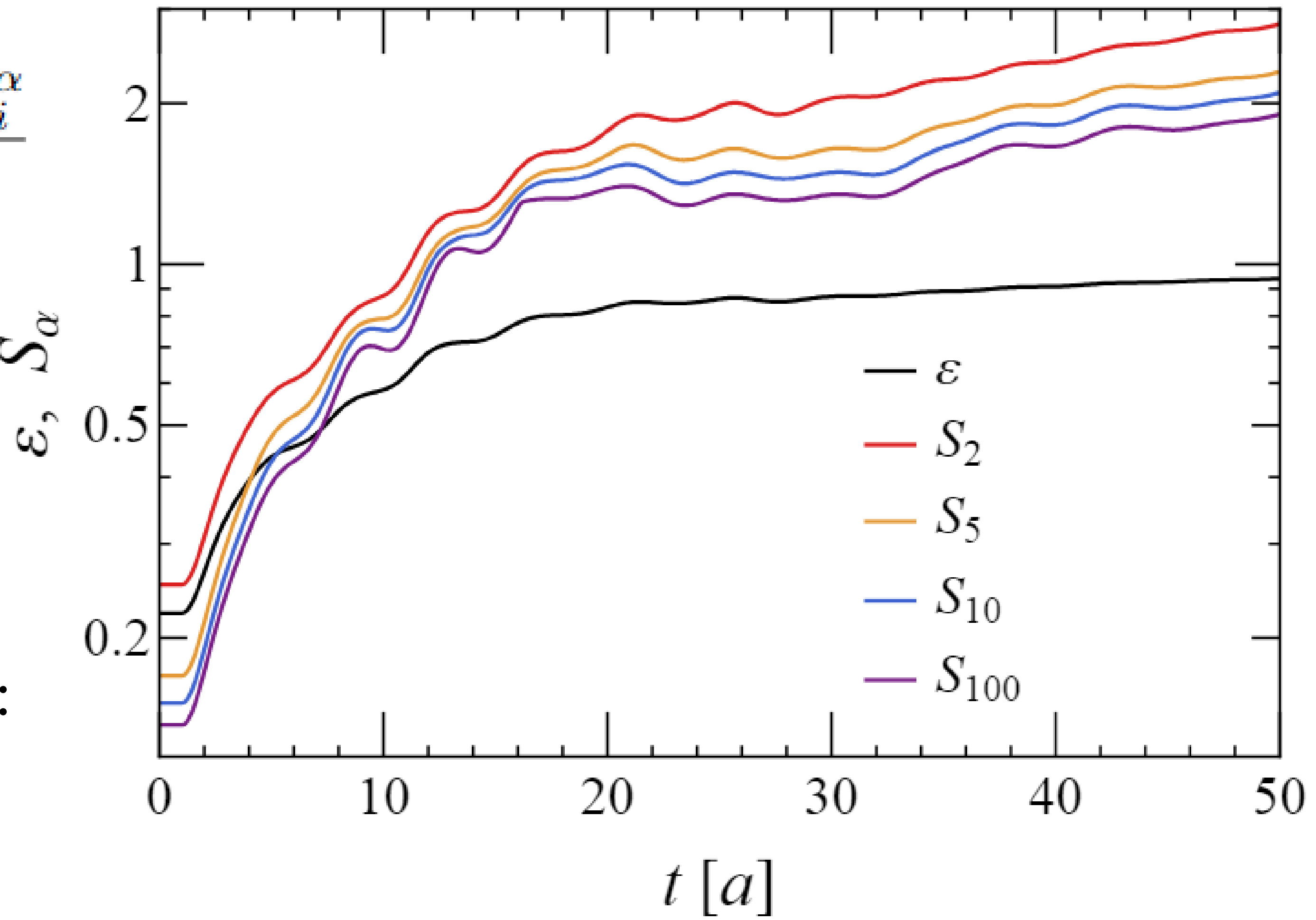

Differentiate between pure state (PS) and maximally entangled state (MES):

$$S_\alpha[\mathrm{PS}] = 0\ , \qquad \mathcal{E}[\mathrm{PS}] = 0$$

$$S_\alpha[\mathrm{MES}] = \frac{N \ln 2}{2}\ \forall\alpha\ , \qquad \mathcal{E}[\mathrm{MES}] = 1$$

Fermionic Fock (computational) basis

$|\mathcal{N}\rangle = |1010\ldots10\rangle$ Neel state

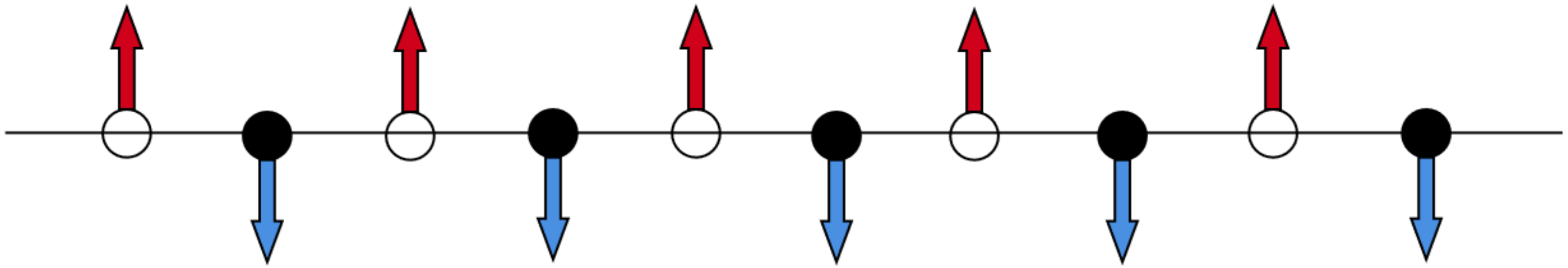

N=10 example

Fermionic Fock (computational) basis

$|\mathcal{N}\rangle = |1010\ldots10\rangle$ Neel state

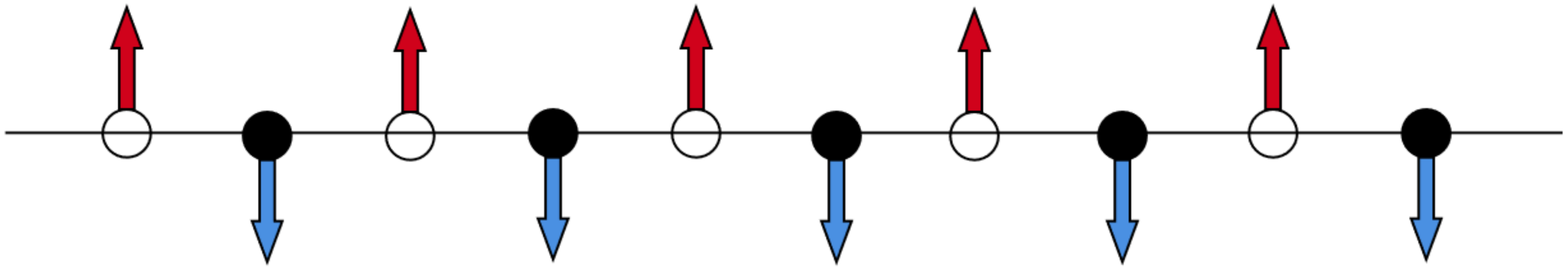

N=10 example

$|i\,j\rangle = X_i X_j |\mathcal{N}\rangle$ 1-pair excitation

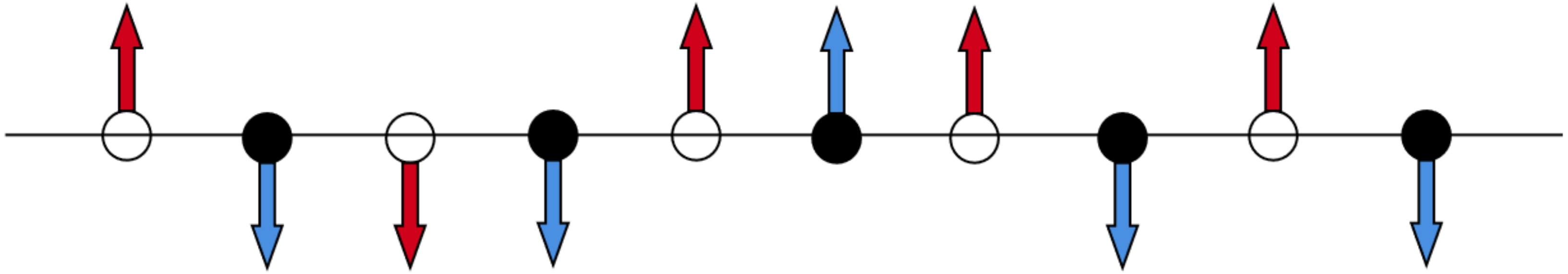

$|3\,6\rangle$ example

…

Hadronization in real time

Maximal overlap

$\max |\langle \psi_L^i(t)|jk\ldots\rangle|$

Schmidt vector

Fock basis state

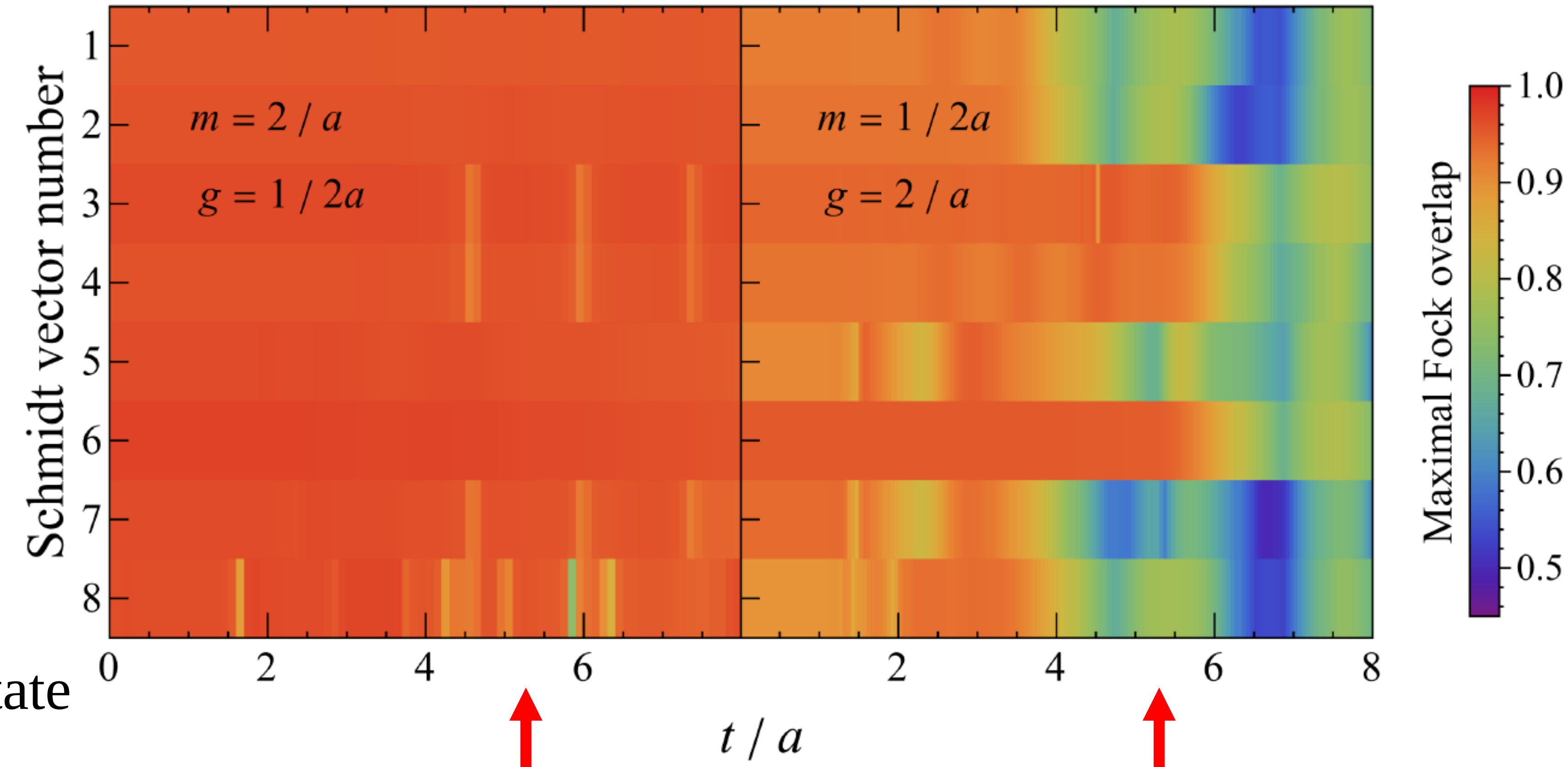

Weak coupling

Strong coupling

Full state overlap with one-pair states

$$p_{i,j} = |\langle \Psi_t | ij \rangle|^2$$

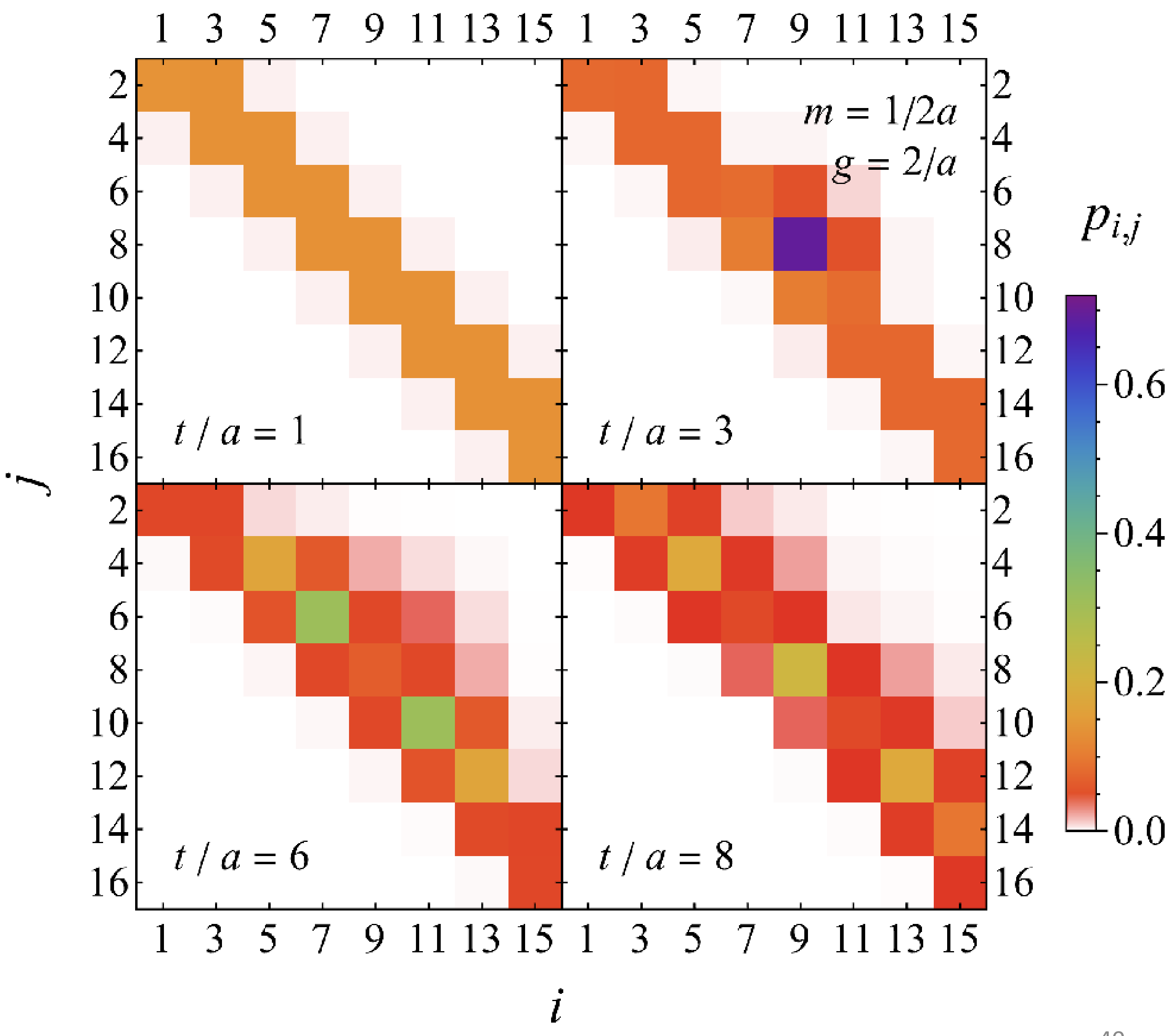

Full state overlap with one-pair states

$$p_{i,j} = |\langle \Psi_t | ij \rangle|^2$$

t/a=3 Nearest neighbor pair - meson

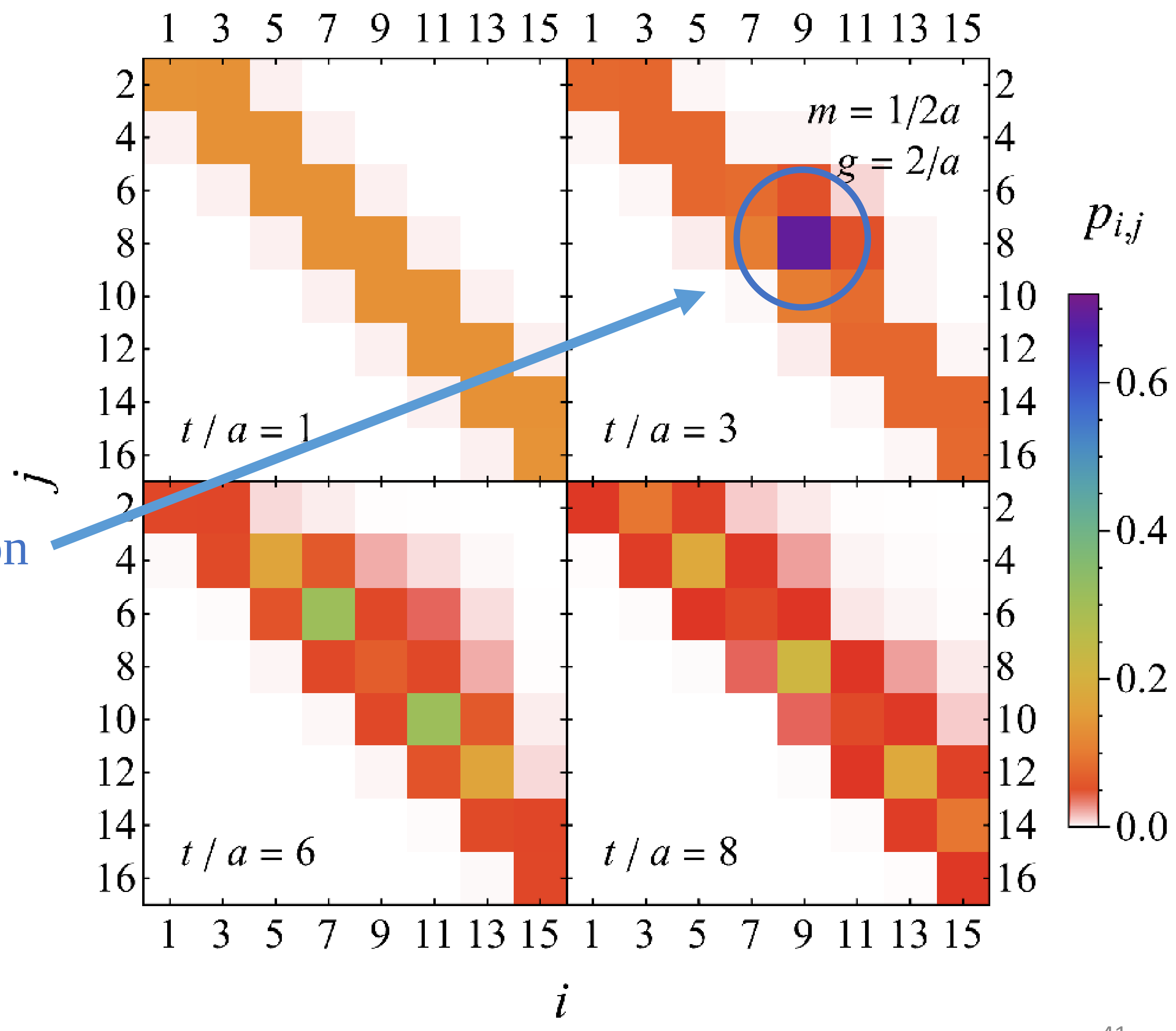

Full state overlap with one-pair states

$$p_{i,j} = |\langle \Psi_t | ij \rangle|^2$$

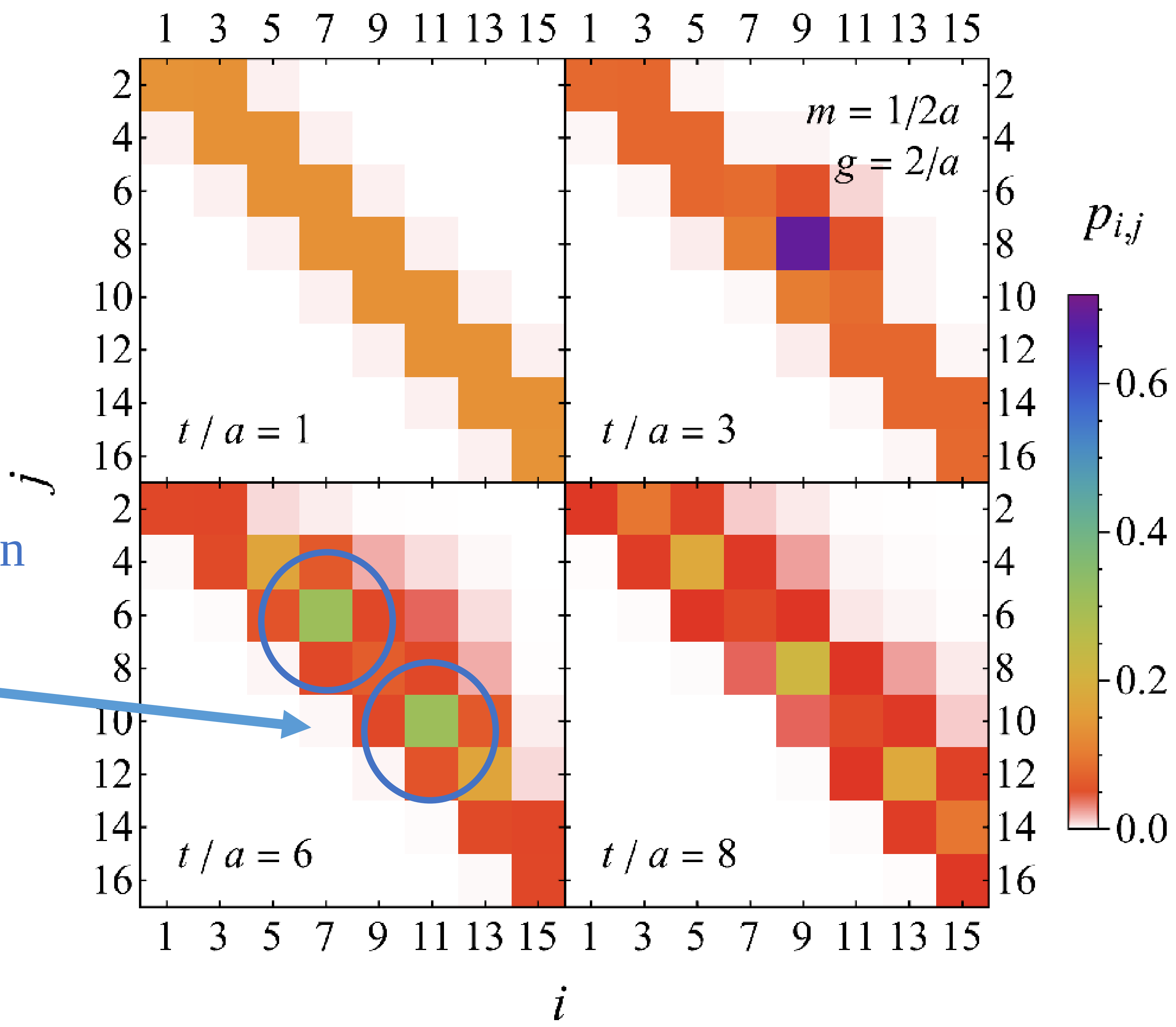

t/a=3 Nearest neighbor pair - meson

t/a=6 – Two mesons

Full state overlap with one-pair states

$$p_{i,j} = |\langle \Psi_t | ij \rangle|^2$$

t/a=3 Nearest neighbor pair - meson

t/a=6 – Two mesons

t/a=8 – Three mesons

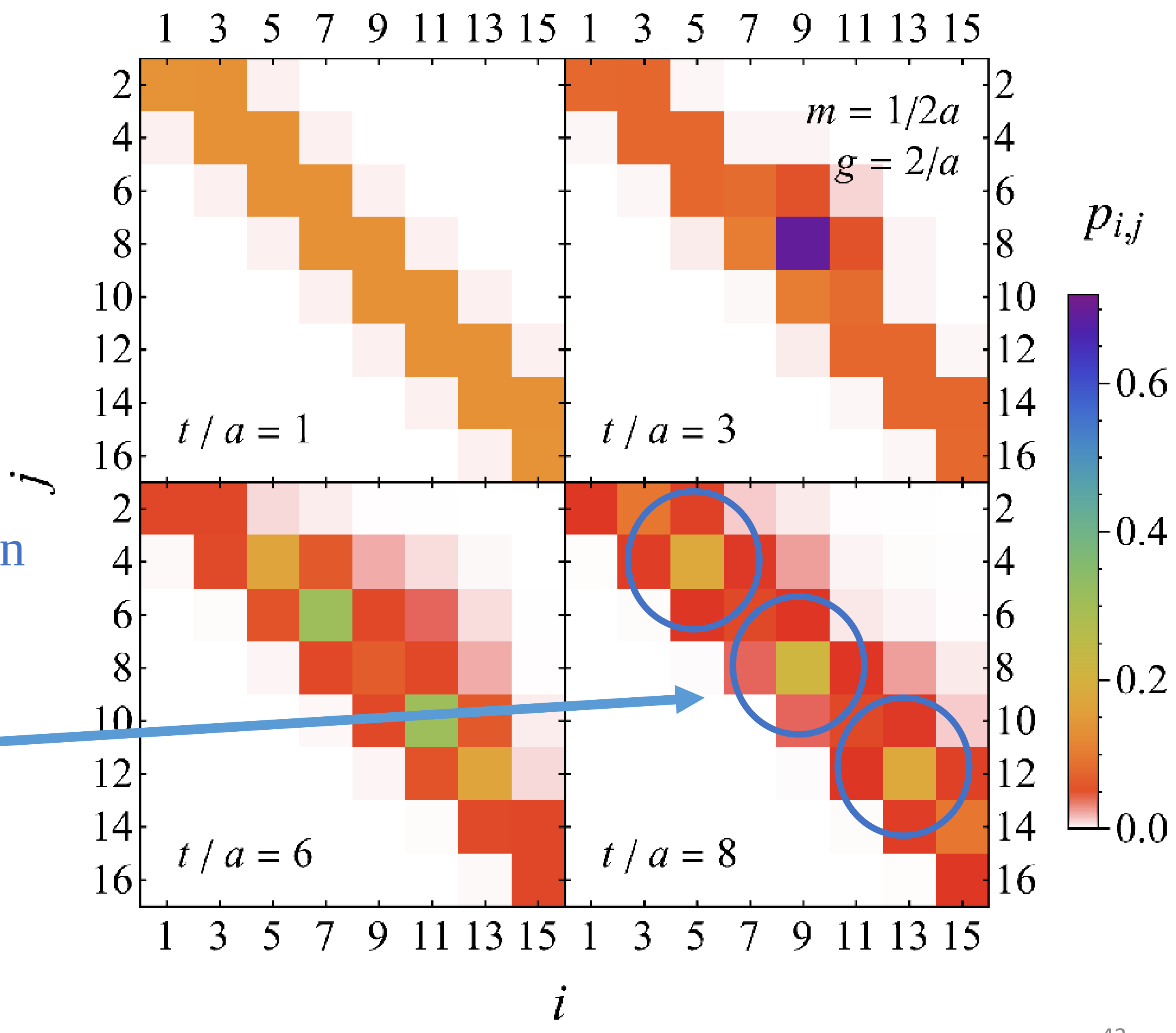

Full state overlap with one-pair states

$$p_{i,j} = |\langle \Psi_t | ij \rangle|^2$$

t/a=3 Nearest neighbor pair - meson

t/a=6 – Two mesons

t/a=8 – Three mesons

……………………

Thermal gas of hadrons?

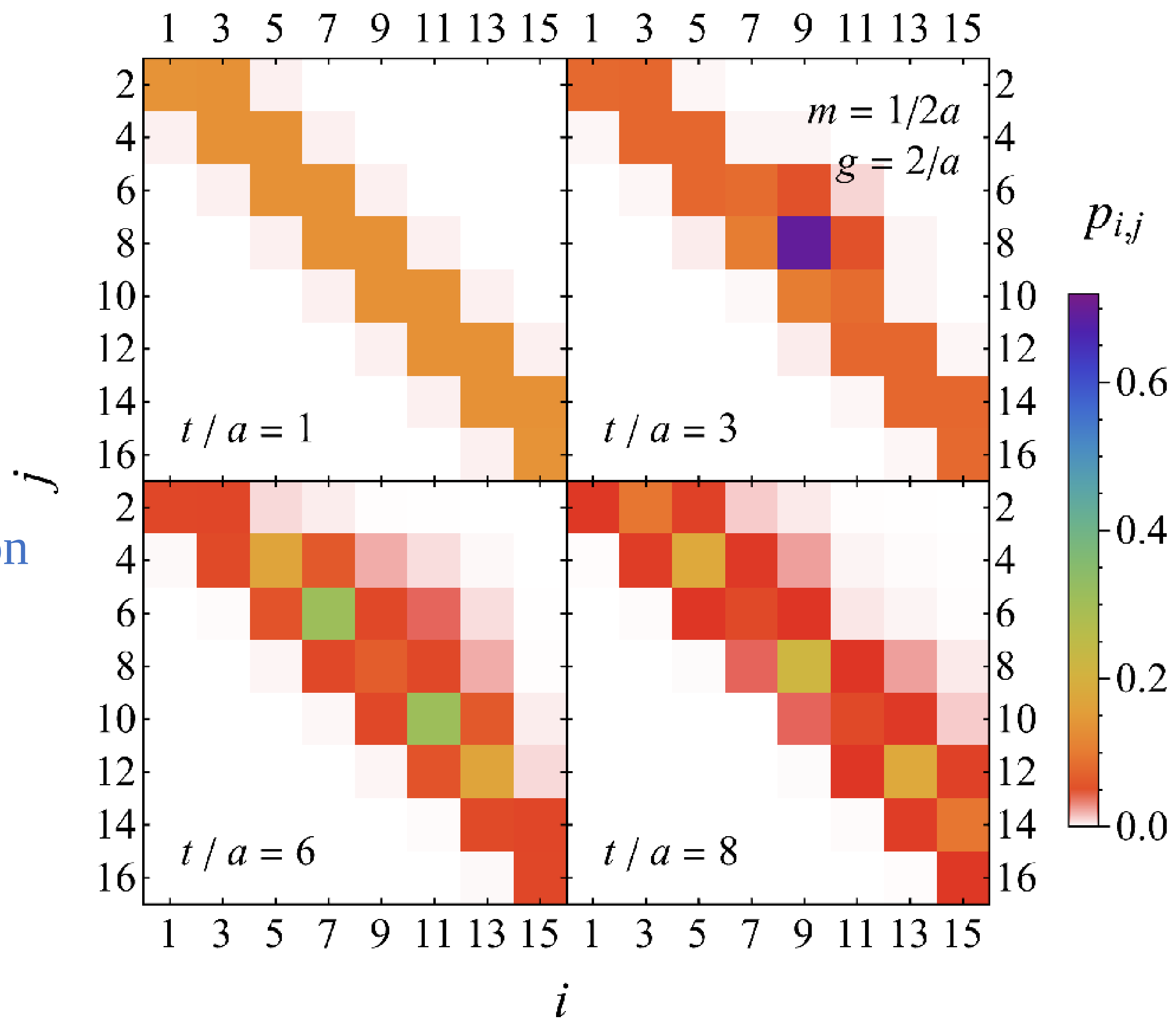

Signal propagation

Modify the external source:

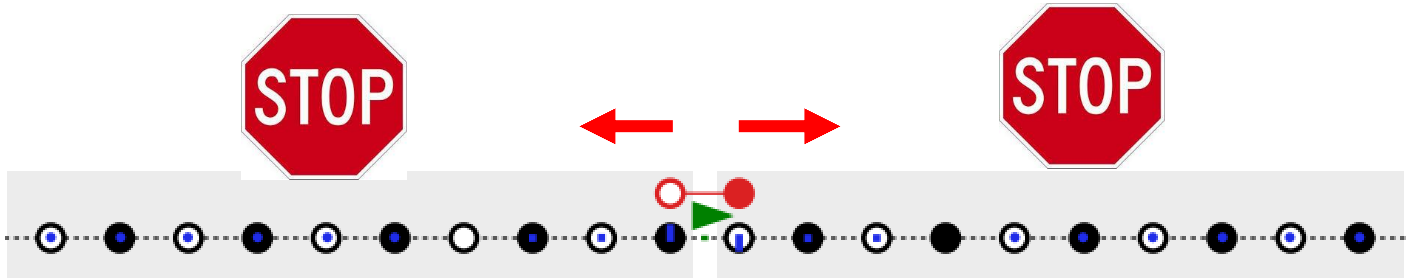

$$L_{\mathrm{ext},n}(t) = \begin{cases} -\theta\left(\frac{t-t_0}{a} - \left|n - \frac{N}{2}\right|\right), & t \leq t_{end} \\ -\theta\left(\frac{t_{end}-t_0}{a} - \left|n - \frac{N}{2}\right|\right), & t > t_{end} \end{cases}$$

instead of

$$L_{\mathrm{ext},n}(t) = -\theta\left(\frac{t-t_0}{a} - \left|n - \frac{N}{2}\right|\right)$$

Compare different t_{end}

Signal propagation

Modify the external source:

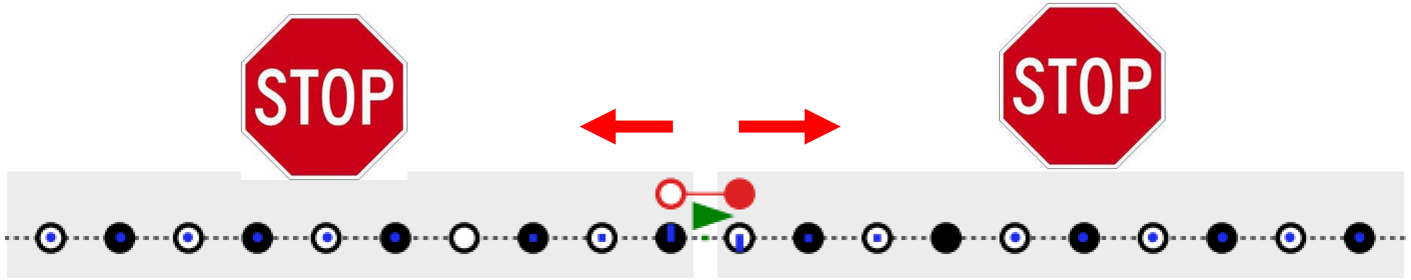

$$L_{\text{ext},n}(t) = \begin{cases} -\theta\left(\frac{t-t_0}{a} - \left|n - \frac{N}{2}\right|\right), & t \leq t_{end} \\ -\theta\left(\frac{t_{end}-t_0}{a} - \left|n - \frac{N}{2}\right|\right), & t > t_{end} \end{cases}$$

instead of

$$L_{\text{ext},n}(t) = -\theta\left(\frac{t-t_0}{a} - \left|n - \frac{N}{2}\right|\right)$$

Compare different t_{end}

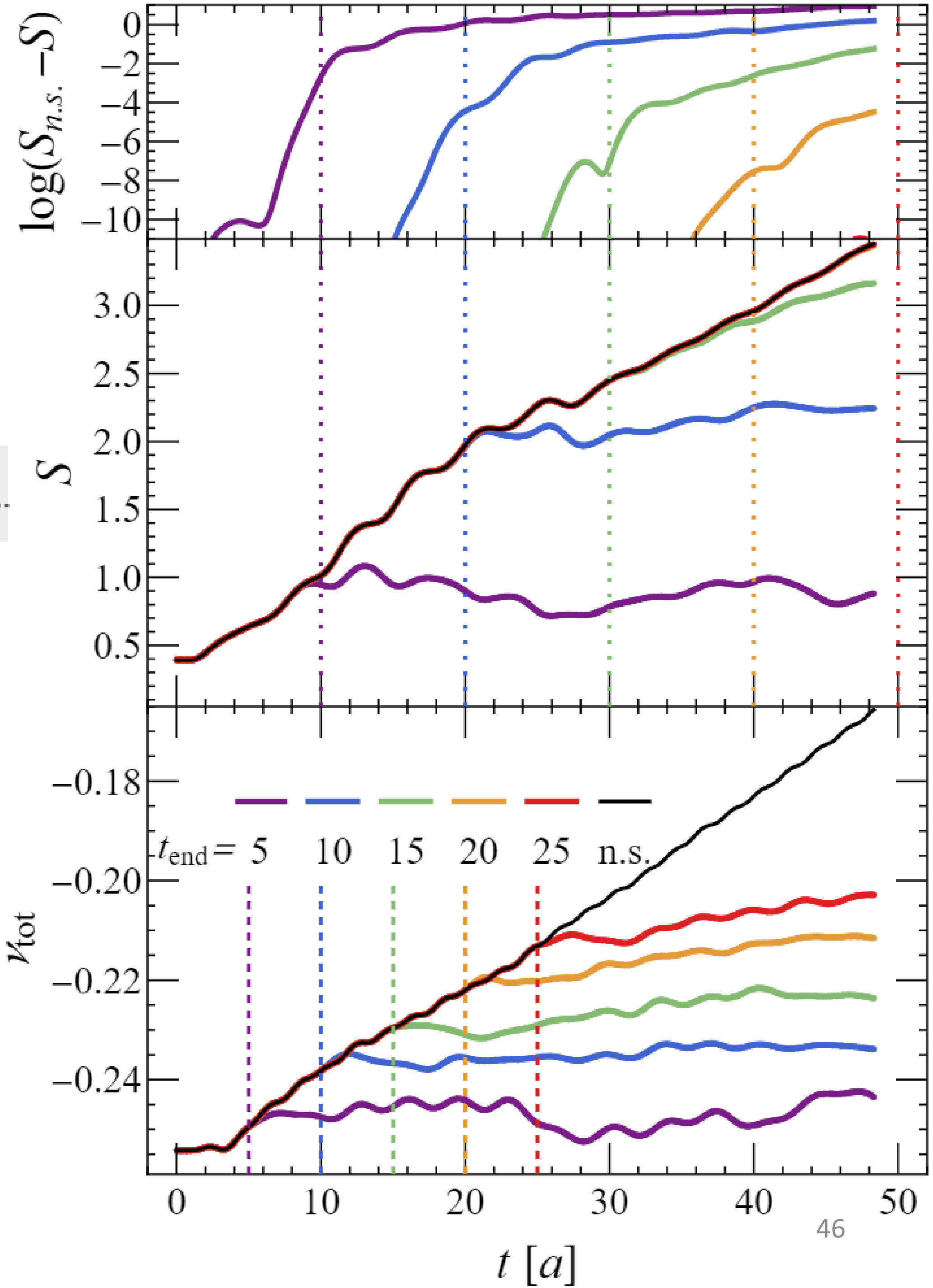

Signal propagation

Modify the external source:

$$L_{\mathrm{ext},n}(t) = \begin{cases} -\theta\left(\frac{t-t_0}{a} - \left|n - \frac{N}{2}\right|\right), & t \le t_{end} \\ -\theta\left(\frac{t_{end}-t_0}{a} - \left|n - \frac{N}{2}\right|\right), & t > t_{end} \end{cases}$$

instead of

$$L_{\mathrm{ext},n}(t) = -\theta\left(\frac{t-t_0}{a} - \left|n - \frac{N}{2}\right|\right)$$

Condensate responds instantaneously

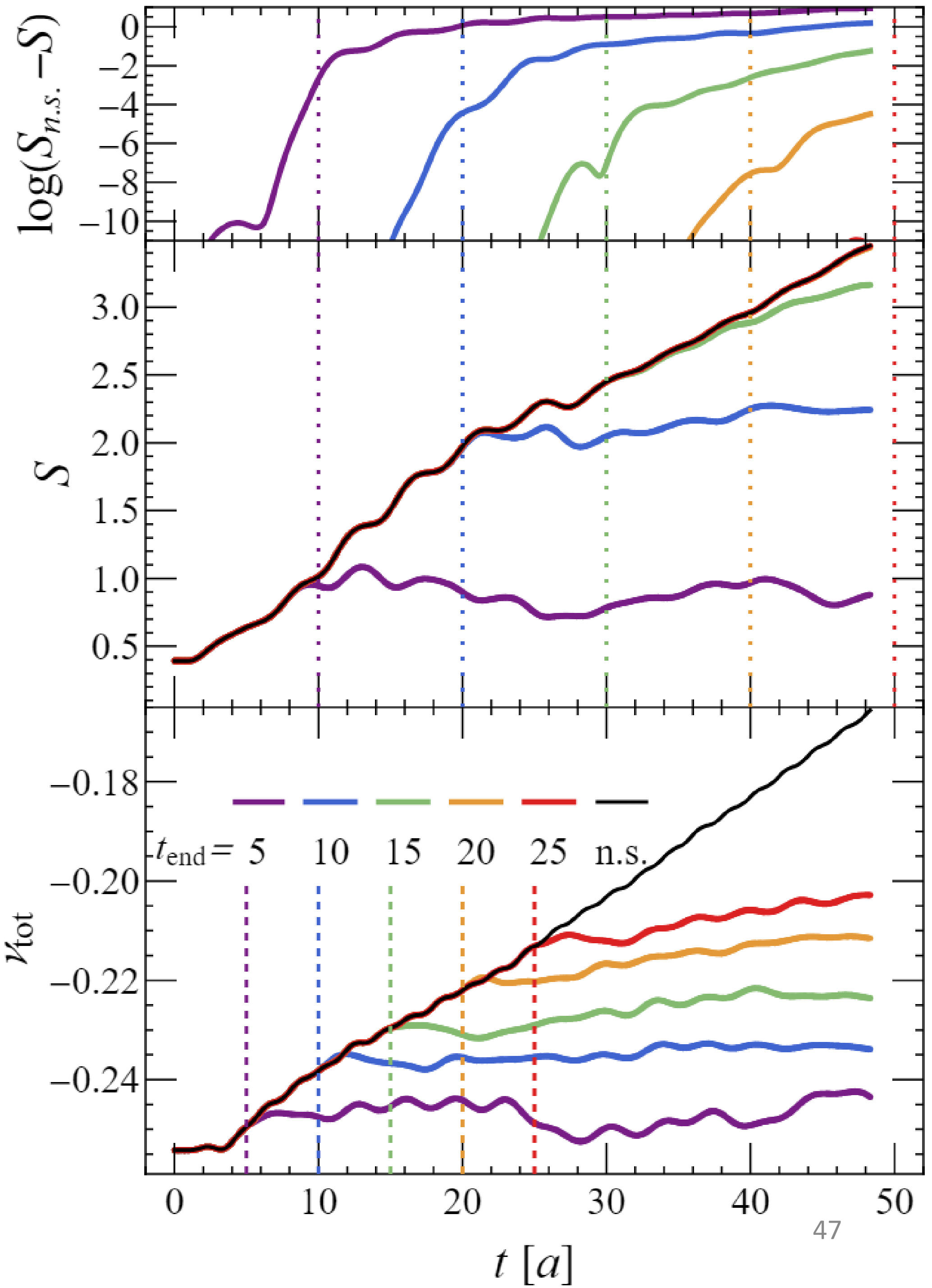

Signal propagation

Entanglement entropy does not deviate until $t \sim 2\, t_{end}$

Information propagates back to the boundary at about speed of light

Condensate responds instantaneously

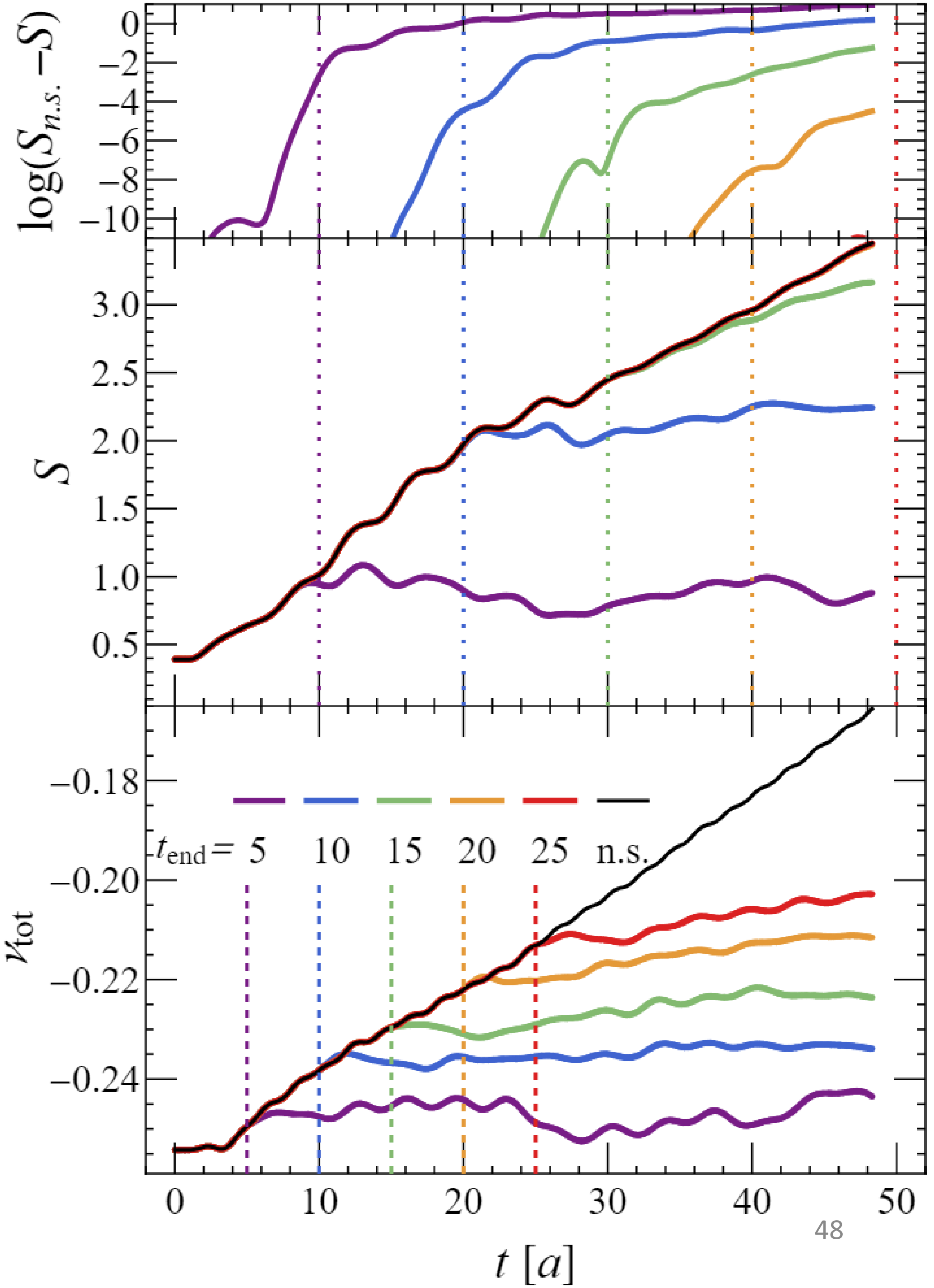

Conclusion

- Dynamical pair production leads to electric field screening and modification of the vacuum condensate
- Local observables thermalize in the central region
- Second Renyi entropy transitions from the area law to the volume law
- Entanglement between jets steadily grows with contributions from many Schmidt states
- At large coupling we observe a dynamical transition of Schmidt states from fermionic Fock states to bosonic Fock states

Outlook

- What determines the effective temperature?
- Is temperature related to the size of maximally entangled subspace?
- Go to higher dimension